JHU/APL
TG 1381
JANUARY 1992

*Technical Memorandum*

# SIMULATING RADAR PROPAGATION THROUGH ATMOSPHERIC TURBULENCE USING THE TROPOSPHERIC ELECTROMAGNETIC PARABOLIC EQUATION ROUTINE (TEMPER)

DANIEL ROUSEFF



THE JOHNS HOPKINS UNIVERSITY ■ APPLIED PHYSICS LABORATORY

UNCLASSIFIED

SECURITY CLASSIFICATION OF THIS PAGE

# REPORT DOCUMENTATION PAGE

| | |
|---|---|
| 1a. REPORT SECURITY CLASSIFICATION<br>Unclassified | 1b. RESTRICTIVE MARKINGS |
| 2a. SECURITY CLASSIFICATION AUTHORITY | 3. DISTRIBUTION/AVAILABILITY OF REPORT<br>Approved for public release; distribution unlimited |
| 2b. DECLASSIFICATION/DOWNGRADING SCHEDULE | |
| 4. PERFORMING ORGANIZATION NUMBER(S)<br>JHU/APL TG 1381 | 5. MONITORING ORGANIZATION REPORT NUMBER(S)<br>JHU/APL TG 1381 |
| 6a. NAME OF PERFORMING ORGANIZATION<br>The Johns Hopkins University Applied Physics Laboratory<br>6b. OFFICE SYMBOL (If Applicable)<br>TIR | 7a. NAME OF MONITORING ORGANIZATION<br>NAVTECHREP/Laurel, Maryland |
| 6c. ADDRESS (City, State, and ZIP Code)<br>Johns Hopkins Road<br>Laurel, Maryland 20723-6099 | 7b. ADDRESS (City, State, and ZIP Code)<br>Johns Hopkins Road<br>Laurel, Maryland 20723-6099 |
| 8a. NAME OF FUNDING/SPONSORING ORGANIZATION<br>Naval Sea Systems Command<br>8b. OFFICE SYMBOL (If Applicable)<br>PMS-400 | 9. PROCUREMENT INSTRUMENT IDENTIFICATION NUMBER<br>N00039-89-C-5301 |
| 8c. ADDRESS (City, State, and ZIP Code)<br>Washington, DC 20362 | 10. SOURCE OF FUNDING NUMBERS<br>PROGRAM ELEMENT NO. / PROJECT NO. / TASK NO. BKAW9BXX / WORK UNIT ACCESSION NO. |

11. TITLE (Include Security Classification)
Simulating Radar Propagation Through Atmospheric Turbulence Using the Tropospheric Electromagnetic Parabolic Equation Routine (TEMPER) (U)

12. PERSONAL AUTHOR(S)
Daniel Rouseff

| 13a. TYPE OF REPORT | 13b. TIME COVERED | 14. DATE OF REPORT (Year, Month, Day) | 15. PAGE COUNT |
|---|---|---|---|
| Technical Memorandum | FROM 4/90 TO 10/91 | 20 November 1991 | 57 |

16. SUPPLEMENTARY NOTATION

| 17. COSATI CODES | | | 18. SUBJECT TERMS |
|---|---|---|---|
| FIELD | GROUP | SUB-GROUP | Radar, Propagation and Scattering, Turbulence, Electromagnetics, Troposphere |
| | | | |
| | | | |

19. ABSTRACT (Continue on reverse if necessary and identify by block number)

The Tropospheric Electromagnetic Parabolic Equation Routine (TEMPER) being developed by the Fleet Systems Department at the Applied Physics Laboratory has proven to be a useful tool in predicting low-altitude radar propagation. A marching procedure is used to step the field through what has been assumed to be a deterministic spatially varying index of refraction profile. In an actual environment, small-scale random fluctuations from atmospheric turbulence are superimposed on the deterministic profile. In this report, a method for coupling random refractivity fluctuations into TEMPER is proposed and tested numerically. Three-dimensional spectral models from the atmospheric literature are used to derive the one-dimensional transverse spectra of refractivity necessary for parabolic simulations. Realizations consistent with the spectra are generated using filtered white noise. Propagation studies are conducted for the canonical problem of a plane wave transmitted through homogeneous isotropic turbulence. Good agreement is observed between the numerical results and existing theory for the second moment of the scattered field. However, the agreement is less good for predicting the random fluctuations in the log-amplitude of the field as three-dimensional effects become significant. Methods for simulating inhomogeneous boundary layer turbulence are considered. The limits of spectral modeling for simulating turbulence are discussed.

| 20. DISTRIBUTION/AVAILABILITY OF ABSTRACT | 21. ABSTRACT SECURITY CLASSIFICATION | |
|---|---|---|
| ☒ UNCLASSIFIED/UNLIMITED ☐ SAME AS RPT. ☐ DTIC USERS | Unclassified | |
| 22a. NAME OF RESPONSIBLE INDIVIDUAL<br>NAVTECHREP Security Officer | 22b. TELEPHONE (Include Area Code)<br>(301) 953-5403 | 22c. OFFICE SYMBOL<br>NAVTECHREP |

DD FORM 1473, 84 MAR

SECURITY CLASSIFICATION OF THIS PAGE

UNCLASSIFIED

JHU/APL
TG 1381
JANUARY 1992

*Technical Memorandum*

# SIMULATING RADAR PROPAGATION THROUGH ATMOSPHERIC TURBULENCE USING THE TROPOSPHERIC ELECTROMAGNETIC PARABOLIC EQUATION ROUTINE (TEMPER)

DANIEL ROUSEFF

THE JOHNS HOPKINS UNIVERSITY ■ APPLIED PHYSICS LABORATORY
Johns Hopkins Road, Laurel, Maryland 20723-6099
Operating under Contract N00039-89-C-5301 with the Department of the Navy

# ABSTRACT

The Tropospheric Electromagnetic Parabolic Equation Routine (TEMPER) being developed by the Fleet Systems Department at the Applied Physics Laboratory has proven to be a useful tool in predicting low-altitude radar propagation. A marching procedure is used to step the field through what has been assumed to be a deterministic spatially varying index of refraction profile. In an actual environment, small-scale random fluctuations from atmospheric turbulence are superimposed on the deterministic profile. In this report, a method for coupling random refractivity fluctuations into TEMPER is proposed and tested numerically. Three-dimensional spectral models from the atmospheric literature are used to derive the one-dimensional transverse spectra of refractivity necessary for parabolic simulations. Realizations consistent with the spectra are generated using filtered white noise. Propagation studies are conducted for the canonical problem of a plane wave transmitted through homogeneous isotropic turbulence. Good agreement is observed between the numerical results and existing theory for the second moment of the scattered field. However, the agreement is less good for predicting the random fluctuations in the log-amplitude of the field as three-dimensional effects become significant. Methods for simulating inhomogeneous boundary layer turbulence are considered. The limits of spectral modeling for simulating turbulence are discussed.

# TABLE OF CONTENTS

# LIST OF FIGURES

# 1. INTRODUCTION AND OVERVIEW

The Tropospheric Electromagnetic Parabolic Equation Routine (TEMPER) has proven to be a useful computational tool for modeling propagation through the troposphere. The routine uses a scalar paraxial approximation to the vector electromagnetic wave equation. The resulting equation can be solved by a marching procedure; given an initial field distribution and a description of the medium, the vertical field distribution can be calculated at arbitrary range. Standard atmospheric models or experimentally derived data are used to quantify the macroscopic features of the index of refraction. When sufficient atmospheric data are available, TEMPER yields generally good agreement with field experiments. (Dockery[1] and Kuttler and Dockery,[2] and the references therein, provide a more detailed discussion of this method.)

In the actual atmosphere, small-scale fluctuations in the index of refraction are superimposed upon the large-scale features. These fluctuations are random and highly chaotic and are caused by atmospheric turbulence. Since the physical scale of the turbulence can range from perhaps 100 m to as little as 1 mm, it is clearly impractical to conduct environmental measurements with sufficient resolution to characterize completely a medium that might extend for many kilometers. Although the magnitude of these perturbations may be small, they can serve to focus and defocus the propagating field. At sufficiently long ranges, the cumulative effect can be significant. Consequently, it is desirable to include the statistical nature of these random perturbations in the propagation model.

This report summarizes the progress to date of an ongoing effort to incorporate random refractivity fluctuations in TEMPER. In the proposed approach, appropriate spectral models for the surface layer turbulence are developed. Individual realizations consistent with the desired spectrum are generated numerically. The field is then propagated through the medium using the parabolic equation/split-step algorithm. By averaging across an ensemble of realizations, the statistical properties of the propagated field are estimated. The numerical simulations presented in this report display excellent agreement with existing theoretical expressions for canonical wave propagation problems. These solutions provide a benchmark for evaluating the numerical algorithm.

Although the parabolic equation method has been widely used in optics and acoustics to study wave propagation through random media, electromagnetic propagation through the troposphere presents a unique set of problems. Unlike the situations typically encountered in optics and acoustics, electromagnetic propagation is usually governed by weak scattering theory. This difference in theoretical approach affects the statistical quantities that are estimated in the numerical simulations. Unlike the spectra in analogous ocean acoustics problems, multidimensional spectral representations for atmospheric turbulence are not separable into the products of simple, one-dimensional spectra. In addition, unlike

---

[1]G. D. Dockery, *Description and Validation of the Electromagnetic Parabolic Equation Propagation Model (EMPE)*, JHU/APL FS-87-152, Applied Physics Laboratory, Laurel, Md. (1987).

[2]J. R. Kuttler and G. D. Dockery, "Theoretical Description of the Parabolic Approximation/Fourier Split-Step Method of Representing Electromagnetic Propagation in the Atmosphere," *Radio Sci* **26**, 381-394 (1991)

the homogeneous turbulence of the free atmosphere usually encountered in optics, surface layer turbulence at low altitudes is inhomogeneous and possibly anisotropic. These features and others have a significant effect on the way in which turbulence is modeled and coupled into a parabolic equation routine.

Section 2 briefly reviews the properties of homogeneous isotropic turbulence and the associated Kolmogorov spectrum. Existing statistical models for atmospheric turbulence are described and modified spectra useful in wave propagation studies are considered. The effects of the turbulent inner and outer scales on the spectrum are noted. The structure constant of turbulence is related to the macroscopic mean refractivity profile. The height-dependent nature of the turbulence for low altitudes is modeled, and the profile used by Levy and Craig[3] in their parabolic equation simulations is presented as a numerical example. The advantages and limitations of spectral modeling for simulating turbulence are discussed.

Section 3 begins by reviewing the classical theories for wave propagation through random media. Both weak and strong scattering theories are discussed. Whereas strong scattering theory is concerned with the statistical moments of the total field, weak scattering theory typically deals with the moments of either the log-amplitude or phase of the field. Existing results for plane wave and point source propagation are summarized. The validity of using two-dimensional simulations such as TEMPER to model three-dimensional propagation through a random medium is studied for a plane wave. It is shown that although two-dimensional modeling often suffices for calculating the moments of the field, it may be inadequate for calculating the log-amplitude fluctuations. A numerical example is given, illustrating the differences between two- and three-dimensional propagation.

Section 4 details how random fluctuations can be included in TEMPER. The transverse spectrum is shown to be the necessary statistical quantity for describing the medium. Analytical expressions for the transverse spectrum of turbulence are derived and presented in terms of special mathematical functions. Simplified expressions valid at microwave frequencies are then deduced and compared to those of Levy and Craig.[3] Numerical realizations of the transverse process are generated and the multiscale properties of turbulence are observed. Results of preliminary wave propagation studies are presented. The three-dimensional effects in the log-amplitude fluctuations predicted in section 3 are confirmed by numerical experiments. Good agreement with three-dimensional theory is obtained for the second moment of the scattered field.

Finally, section 5 summarizes the main results of this study. A program for upgrading TEMPER by including random refractivity fluctuations is proposed.

---

[3]M. F. Levy and K. H. Craig, "Millimetre-Wave Propagation in the Evaporation Duct," in *Atmospheric Propagation in the UV, Visible, IR and MM-Wave Region and Related Systems Aspects*, AGARD Conf. Proc 454, Neuilly-sur-Seine, France, pp. 26.1-26.10 (1989).

# 2. STATISTICAL MODELS FOR ATMOSPHERIC TURBULENCE

In contrast to steady laminar flow, turbulence is chaotic and characterized by random, highly rotational motion. Atmospheric parameters such as wind speed, temperature, humidity, and pressure can all exhibit turbulent fluctuations. Since some of these quantities determine the index of refraction, an electromagnetic wave propagating through a turbulent medium will also acquire random variations. To predict the statistical nature of the field fluctuations, it is necessary to describe the statistical properties of the medium through which it propagates.

This section will emphasize the use of existing spectral models for turbulent fluctuations in the index of refraction. The spectral modeling approach is attractive for several reasons. For the theorist, existing wave propagation theories are usually formulated in terms of the spectrum of the random medium. For the experimentalist, spectra can often be quantified by a limited number of observable parameters. Spectral models are also easy to implement numerically; to simulate realizations of an assumed Gaussian random process, all that is required is a random number generator and a fast Fourier transform (FFT) routine. The approach can be adapted to temporal spectra and to spatial spectra of any number of dimensions. Finally, of particular relevance to upgrading TEMPER, the spectral approach has already been extensively applied in conjunction with the split-step algorithm to study acoustic propagation through a random ocean.

## 2.1 LOCALLY HOMOGENEOUS ISOTROPIC TURBULENCE

Turbulence is a cascade process whereby large-scale eddies are broken into successively smaller sizes until they are eventually dissipated in the form of heat. The outer scale, $L_0$, for turbulence in the free atmosphere typically ranges from 10 to 100 m. The inner scale, $\ell_0$, also called the Kolmogorov microscale, is on the order of millimeters or centimeters. Eddies larger than $L_0$ feed energy into the turbulence. Between the two extremes, the eddies are said to be in the inertial subrange, where the kinetic energy of the eddies dominates the dissipative effects. Structures less than $\ell_0$ are quickly dissipated owing to viscosity.

Fully developed turbulence is represented by the Kolmogorov spectrum. Since fully developed turbulence is isotropic, the three-dimensional spectrum of the index of refraction $S_n$ can be written as a function of a single variable $K$, where $K^2 = k_x^2 + k_y^2 + k_z^2$ and $k_x, k_y$, and $k_z$ represent the spatial frequency components in the different directions. As shown in Figure 2.1, the spectrum can be divided into three regimes. No general expression applies for spatial frequencies $0 < K < 2\pi / L_0$, where energy is input into the turbulence. Within the inertial subrange $2\pi / L_0 < K < 2\pi / \ell_0$, the spectrum is described by a power law and goes like $K^{-11/3}$. In the dissipation range, the spectrum falls rapidly to zero.

In practice, meteorological parameters are often measured as a function of a single spatial variable from which one-dimensional spectra $V(K)$ are estimated. Since for an isotropic process the three-dimensional spectrum is also a function of a single variable, the two spectra for the refractive index $n$ are related by (see Ref. 4, p. 517)

---

[4]A. Ishimaru, *Wave Propagation and Scattering in Random Media*, Academic Press, New York (1978).

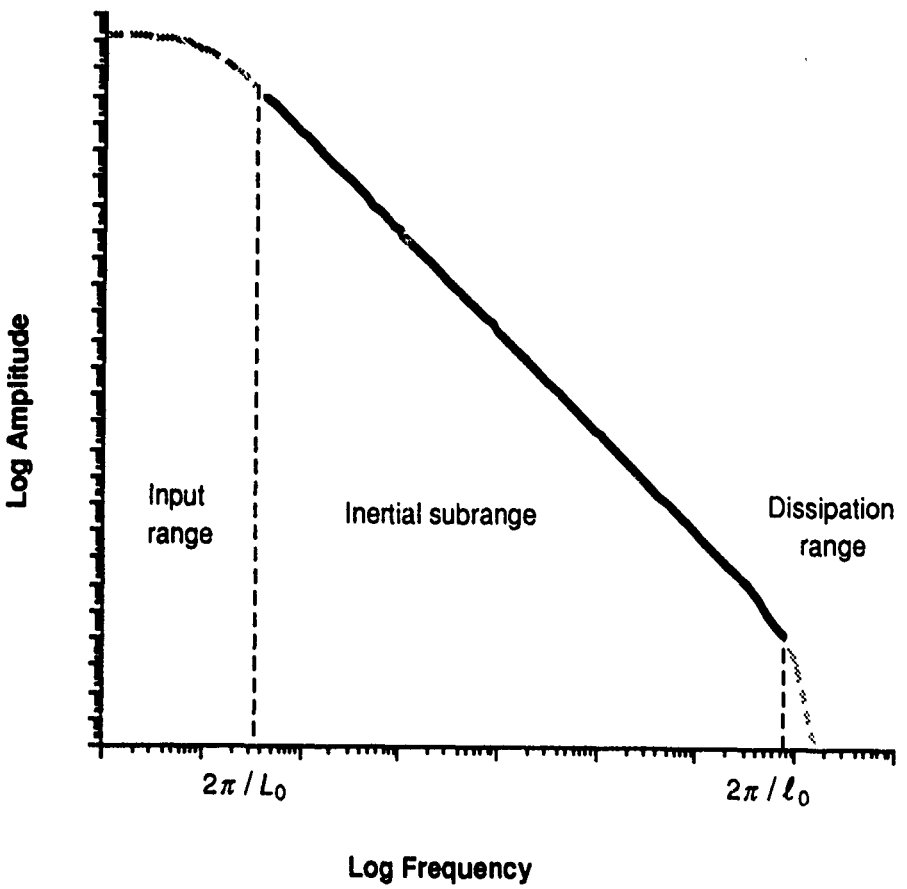


**Figure 2.1** Kolmogorov spectrum for turbulence. Spatial frequencies $0 < K < 2\pi/L_0$, where $L_0$ is the outer scale, constitute the energy input region. No general form for the spectrum exists in this range. The inertial subrange is bounded by $2\pi/L_0 < K < 2\pi/\ell_0$, where $\ell_0$ is the inner scale of the turbulence. Within this region, the three-dimensional spectrum is proportional to $K^{-11/3}$. The spectrum rapidly decreases in the dissipation region, where $K > 2\pi/\ell_0$.

$$S_n(K) = \frac{-1}{2\pi K} \frac{\partial V_n(K)}{\partial K}. \qquad (2.1)$$

Consequently, $V_n$ is proportional to $K^{-5/3}$ in the inertial subrange. The transverse spectrum, which is also one-dimensional but obeys a different power law, is defined in section 4.1. It will be shown that the transverse spectrum and not $V_n(K)$ is of relevance for including turbulent fluctuations in TEMPER simulations.

Usually, a spectrum is related to a correlation function by a Fourier transform pair through the Wiener-Khinchin theorem. For this transform pair to exist, the process must be statistically homogeneous. Statistical homogeneity is an extension of the familiar time series concept of wide sense stationarity to multiple spatial dimensions.[5] A statistically homogeneous process will have a constant mean and its autocorrelation will depend only on the distance between the points being correlated and not on the absolute position. Unfortunately, atmospheric turbulence is not statistically homogeneous, since both of the mean characteristics will fluctuate in space and the correlation function will depend on position. The lack of homogeneity is reflected in the Fourier domain by the spectrum being undefined for frequencies $0 < K < 2\pi/L_0$. To circumvent these difficulties, Kolmogorov extended the concept of stationarity to define a process that is locally homogeneous. He noticed that although the wind velocity is not homogeneous, the difference between the wind velocities taken at points less than $L_0$ apart will behave like a homogeneous process. This locally homogeneous process is called a structure function. Denoting the three-dimensional position vector by $\mathbf{r}$, the structure function $D_n$ of the index of refraction is

$$D_n(\mathbf{r}) = \left\langle \left| n(\mathbf{r}_1 + \mathbf{r}) - n(\mathbf{r}_1) \right|^2 \right\rangle, \qquad (2.2)$$

where the angle brackets indicate an ensemble average. If the process is also isotropic, then $D_n = D_n(r)$, where $r = |\mathbf{r}|$. For an isotropic, locally homogeneous Kolmogorov process, the structure function is given by

$$D_n(r) = C_n^2 r^{2/3} \qquad \text{for} \quad L_0 >> r >> \ell_0 \qquad (2.3a)$$

$$D_n(r) = C_n^2 \ell_0^{2/3} (r/\ell_0)^2 \qquad \text{for} \quad r << \ell_0, \qquad (2.3b)$$

where $C_n$ is the structure constant. Equation 2.3a is a statement of the well-known "Kolmogorov two-thirds law" that permeates the turbulence literature. The structure function is not explicitly defined for distances greater than $L_0$, which acts like the correlation length of the medium. For distances greater than the correlation length, however, $n(\mathbf{r}_1+\mathbf{r})$ and $n(\mathbf{r}_1)$ in Equation 2.2 will become

[5] A. J. Devaney, "The Inverse Problem for Random Sources," *J Math Phys.* **20**, 1687-1691 (1979).

essentially uncorrelated and the structure function will become related to the variance of the process. Finally, the structure function of an isotropic process is related to the spectrum by

$$D_n(r) = 8\pi \int_0^\infty [1 - (Kr)^{-1} \sin(Kr)] S_n(K) K^2 \, dK \qquad (2.4)$$

(see Ref. 4, p. 524). Note from Equation 2.4 that spatial frequencies $K < 2\pi/L_0$ make minimal contributions to the integration for $r \ll L_0$ and reasonable spectra; consequently, the structure function and the spectrum can be related by a transform pair even when $S_n$ is not well known for low frequencies.

## 2.2 MODIFIED SPECTRAL REPRESENTATIONS

Figure 2.1 shows three separate spectral regimes for turbulence with the energy input regime undefined. For mathematical convenience, it is often useful in wave propagation theory to assign a spectral shape to the input regime and then to combine all three regimes into a single function. The resulting expression is the so-called von Karman spectrum (see Ref. 4, p. 337, and Ref. 6, p. 5),

$$S_n(K) = 0.033 C_n^2 \left(K^2 + L_0^{-2}\right)^{-11/6} \exp\left(-K^2 / K_m^2\right), \qquad (2.5)$$

where $K_m = 5.92/\ell_0$. Equation 2.5 must be considered an approximate representation of turbulence, since the spectral shape for low frequencies is unknown. The von Karman spectrum is a well behaved function that has a conventional inverse Fourier transform and hence a function that can be interpreted as the autocorrelation; the von Karman spectrum consequently can describe a process that is both locally homogeneous and statistically homogeneous. These distinctions between locally homogeneous and statistically homogeneous processes are subtle and are discussed in further detail by Ishimaru[4] and Tatarskii.[7] The main point is that if the von Karman spectrum is used in any wave propagation analysis, the resulting solutions for the statistics of the field are at best reliable only for correlation distances less than the outer scale of the medium.

Kolmogorov's original insights were based on dimensional analysis and the assumption that the turbulence is isotropic. For well developed turbulence far from any boundaries, the isotropic assumption is usually valid. At low altitudes, however, turbulence becomes anisotropic. For example, as mentioned in section 1, a typical value for the outer scale in free turbulence is 100 m. At altitudes less than 100 m, the horizontal outer scale might remain unchanged, but the vertical correlation scale must be reduced. The Kolmogorov spectrum can be modified to model an anisotropic process yielding (Ref. 4, p. 339)

---

[6]B. J. Uscinski, *The Elements of Wave Propagation in Random Media*, McGraw-Hill, New York (1978).

[7]V. I. Tatarskii, *The Effects of the Turbulent Atmosphere on Wave Propagation*, Keter Press, Jerusalem (1971).

$$S_n(k_x,k_y,k_z) = 0.033C_n^2\left(k_x^2\ell_x^2 + k_y^2\ell_y^2 + k_z^2\ell_z^2\right)^{-11/6}(\ell_x\ell_y\ell_z)^{11/3}, \quad (2.6)$$

where $\ell_x$, $\ell_y$, and $\ell_z$ are the outer scales in the three directions. The lowest 100 m of the atmospheric boundary layer, where turbulence is often anisotropic, is called the surface layer.[8,9] Equation 2.6 is valid in the inertial subrange. Presumably, some hybrid of Equations 2.5 and 2.6 could be developed to yield a complete spectral representation of anisotropic surface layer turbulence.

For simplicity, the isotropic model of Equation 2.5 will be used in the majority of this report. This is done with the understanding that a parallel development is possible for the anisotropic model should it prove necessary.

A further complicating factor is that the "structure constant" $C_n$ is, in fact, not constant for altitudes in the surface layer. This is discussed in further detail in section 2.3.

## 2.3 STRUCTURE CONSTANT AND SURFACE LAYER TURBULENCE

The structure constant $C_n$ determines the strength of the turbulence. In the free atmosphere, it ranges typically between $10^{-7}$ $m^{-1/3}$ for strong turbulence and $10^{-9}$ $m^{-1/3}$ for weak fluctuations. If the turbulence is approximated by a homogeneous process by assuming the von Karman spectrum, $C_n$ can be related to the variance of the random part of the index refraction fluctuations $< n_f^2 >$ and the outer scale (Ref. 4, p. 543):

$$C_n^2 = 1.91\left\langle n_f^2 \right\rangle L_0^{-2/3}. \quad (2.7)$$

Clearly, the numerical determination of the structure constant for a given wave propagation problem is of crucial importance; as will be shown in a later section, the solution for the electromagnetic field fluctuations will be specified in terms of $C_n^2$. One approach to calculating $C_n^2$ begins by specifying the index of refraction in terms of the measurable meteorological parameters. A standard expression for the microwave index of refraction is

$$n - 1 = \frac{77.6}{T}(P + 4810e/T)\times 10^{-6}, \quad (2.8)$$

where $T$ is the temperature in degrees Kelvin, $P$ is the pressure in millibars, and $e$ is the water vapor pressure in millibars. Rather than use the index of refraction, meteorologists prefer to use the potential index of refraction and write an analogous expression in terms of the potential temperature and the potential vapor pressure

---

[8]H. A. Panofsky and J. A. Dutton, *Atmospheric Turbulence Models and Methods for Engineering Applications*, John Wiley and Sons, New York (1984).

[9]Z. Sorbjan, *Structure of the Atmospheric Boundary Layer*, Prentice Hall, Englewood Cliffs, N. J. (1989).

(specific humidity).[10] These potential functions are called conservative passive additives. Unlike $T$ and $e$, a volume element of a conservative passive additive preserves its value as it moves through space, and it does not exchange energy with the turbulence. If we are only interested in refractivity at a constant height, no distinction is necessary.[11]

The index of refraction is written as the sum of a mean deterministic part $<n>$ that may vary slowly in height and range owing to atmospheric stratification, and by a small, randomly fluctuating part $n_f$ due to turbulence. By expanding Equation 2.8, $n_f$ can be written in terms of small perturbations in temperature, pressure, and humidity. The variance of the randomly fluctuating part of the index of refraction can thus be expressed as a function of the variances of the individual meteorological parameters along with certain cross terms that include coupling between the atmospheric variables; for example, temperature and humidity fluctuations are usually correlated. The result is an expression for $C_n^2$ in terms of the presumably measurable structure constants of the meteorological parameters; various expressions are available in the literature.[8,11-14] The relative importance of the various terms depends on the atmospheric conditions, the altitude of interest, and the frequency of the probing wave. The structure constant at optical frequencies is primarily a function of temperature fluctuations, whereas in the microwave range both the humidity and the coupling between temperature and humidity must be considered.

If the mean profile of the index of refraction is known (presumably by measuring the atmospheric parameters), $C_n^2$ can be written in terms of the outer scale of the turbulence and the gradient of the mean profile. Tatarskii[7] gives

$$C_n^2 = a^2 \alpha' L_0^{4/3} (\partial < n > / \partial z)^2 , \qquad (2.9)$$

where $z$ is the height and $\alpha'$ is a correction term. The constant $a^2$ is taken to be a "universal constant" but its precise value is not well known. Various estimates place it between 1.5 and 3.5. For the atmospheric boundary layer, Sorbjan[9] uses 1.6. Ishimaru[4] follows Monin and Yaglom[15] and uses 2.8. In a series of papers, Gossard[11,12,16] uses 3.2. Panofsky and Dutton[8] make no pretense of knowing this "universal constant" to any more than one significant figure and use 3. The correction term $\alpha'$ suggested by Tatarskii is invariably taken to be 1.

---

[10]D. E. Kerr (ed.), *Propagation of Short Radio Waves*, Dover, New York (1951).

[11]E. E. Gossard, "Clear Weather Meteorological Effects on Propagation at Frequencies above 1 GHz," *Radio Sci.* **16**, 589-608 (1981).

[12]E. E. Gossard, "Refractive Index Variation and Its Height Distribution in Different Air Masses," *Radio Sci.* **12**, 89-105 (1977).

[13]S. D. Burk, "Temperature and Humidity Effects on Refractive Index Fluctuations in Upper Regions of the Convective Boundary Layer," *J. Appl. Meteorol.* **20**, 717-721 (1981).

[14]E. L. Andreas, "Estimating $C_n^2$ Over Snow and Sea Ice from Meteorological Data," *J. Opt. Soc Am. A. Opt Image Sci.* **5**, 481-495 (1988).

[15]A. S. Monin and A. M. Yaglom, *Statistical Fluid Mechanics*, MIT Press, Cambridge, Mass. (1971).

[16]E. E. Gossard, "The Height Distribution of Refractive Index Structure Parameter in an Atmosphere Being Modified by Spatial Transition at Its Lower Boundary," *Radio Sci.* **13**, 489-500 (1978).

Even if the mean profile is well known and a reasonable value for $a^2$ is selected, it is still difficult to calculate $C_n^2$ by means of Equation 2.9, owing to its dependence on the outer scale $L_0$. As noted by Van Zandt et al.,[17] the outer scale is notoriously difficult to measure, although the outer scale for turbulence in the free atmosphere is usually taken to be between 10 and 100 m. By examining the backscatter from free atmosphere turbulence, Van Zandt estimated that, on average, $L_0 \cong 10$ m.

For altitudes less than about 100 m, the turbulence can no longer be assumed to be locally homogeneous and isotropic. A first-order expression for the outer scale as a function of height $z$ is

$$L_0 = k_a z \phi^{3/2} \phi_\varepsilon^{-1/4}, \tag{2.10}$$

where $k_a$ is von Karman's constant, $\phi$ is the normalized wind sheer, and $\phi_\varepsilon$ is the normalized dissipation. The von Karman constant is traditionally taken to be 0.4, with values measured in the wind tunnel and the atmosphere ranging from 0.35 to 0.43 (see Ref. 8, p. 122, and Ref. 9, p. 73). For a neutral atmosphere, the normalized parameters are equal to 1. Panofsky and Dutton[8] give formulas for the parameters in both stable and unstable conditions. Combining Equations 2.9 and 2.10 and setting $\alpha' = 1$ yields the structure constant in the boundary layer:

$$C_n^2 = a^2 (k_a z)^{4/3} \phi^{-2} \phi^{-1/3} (\partial < n > / \partial z)^2 . \tag{2.11}$$

## 2.4 NUMERICAL EXAMPLE: PROFILE OF LEVY AND CRAIG

The ultimate goal of this study is to generate numerical realizations of atmospheric turbulence and then do wave propagation studies using the parabolic equation. A similar study was attempted by Levy and Craig.[3] In order to eventually compare numerical results, we now calculate the structure constant for the index of refraction profile used in their study.

Referencing a report by Battaglia,[18] and after converting from modified refractivity to the index of refraction, Levy and Craig use as their profile

$$< n(z) > -1 = 10^{-6} (\alpha - 10^6 / a_c)\, z - \alpha d 10^{-6} \log\left(\frac{z + z_0}{z_0}\right), \tag{2.12}$$

where $a_C$ is the radius of the Earth and $10^6/a_C = 0.157$ m$^{-1}$, $\alpha$ is approximately 0.120 M-units per meter for standard conditions, $d$ is the duct height, and $z_0$ is the

---

[17]T. E. Van Zandt, J. L. Green, K S. Gage, and W. L. Clark, "Vertical Profiles of Refractivity Turbulence Structure Constant: Comparison of Observations by the Sunset Radar with a New Theoretical Model," *Radio Sci* **13**, 819-829 (1978).

[18]M. R Battaglia, *Modelling the Radar Evaporative Duct*, Department of Defence, Defence Science and Technology, RAN Research Laboratory, Australia (1985).

"momentum roughness length." Levy and Craig set a numerical value $z_0 = 1.5 \times 10^{-4}$ m, which is consistent with a calm open sea. (Panofsky and Dutton have tabulated values of $z_0$ for various sea states and terrains [see Ref. 8, p. 123].) Taking the derivative of Equation 2.12 and substituting the numerical constants yields

$$\frac{\partial < n >}{\partial z} = \left[ \frac{-0.120d}{z + z_0} - 0.037 \right] 10^{-6}, \tag{2.13}$$

assuming a natural logarithm in Equation 2.12. Substituting Equation 2.13 into Equation 2.11 gives the structure function. For heights $z_0 << z < d$, $z_0$ and the height-independent part of Equation 2.13 can be neglected. Setting $\phi = \phi_\varepsilon = 1$ yields

$$C_n^2(z) \cong a^2 k_a^{4/3} (0.120d)^2 z^{-2/3} 10^{-12}, \tag{2.14}$$

which agrees with the corrected equation given by Levy and Craig. (Levy and Craig erroneously neglect the factor $10^{-12}$ in their equation, but include it in their subsequent figures.) Equation 2.14 shows the familiar $z^{-2/3}$ dependence characteristic of the atmospheric surface layer.[14] Clearly, however, Equation 2.14 is valid only over a limited regime; near the surface, $z_0$ becomes important to avoid the singularity at $z = 0$, and for $z \gtrsim d$ the constant part of Equation 2.13 should be included.

Although Levy and Craig present plots of the transmission loss versus height and range only up to 20 m, it is interesting to consider the behavior of the structure constant at higher altitudes outside the surface area. Above the boundary layer, the outer scale is approximately constant for $z >> d$ and Equation 2.9 reduces to

$$C_n^2 = (2.8) L_0^{4/3} (0.037)^2 10^{-12}. \tag{2.15}$$

Equating Equations 2.7 and 2.15 relates the variance of the medium to the outer scale:

$$\left\langle n_f^2 \right\rangle = 2.0 \times 10^{-15} L_0^2. \tag{2.16}$$

A typical value of the variance is $10^{-12}$, which gives an outer scale of 22 m and is within the range of acceptable values.

## 2.5 LIMITS OF SPECTRAL MODELING

As discussed in section 2, the spectral modeling approach for generating numerical realizations of turbulence has a number of attractive features. It has also been the traditional method used in conjunction with the parabolic equation.[19] It is not, however, without certain drawbacks and limitations. These limitations and prospective alternative approaches are considered in the discussion that follows.

In the proposed spectral approach for generating realizations, a Gaussian white noise process is first generated using a random number generator. The resulting process is then filtered in accordance with the desired spectrum to yield a Gaussian process. The details of this procedure are given in Appendix A. It is well known from probability theory that a Gaussian process is completely characterized by its second moment and associated spectrum.[20] Consequently, when used with the parabolic equation method, this should produce reasonable results for the second-order statistics of the propagating field.

Unfortunately, atmospheric turbulence is typically an intermittent phenomena obeying non-Gaussian statistics; areas of strong turbulence may be surrounded by quiescent regions. Incorporating these features in a model could be crucial if the objective of a numerical study is to identify potentially catastrophic events and to assign a probability to their occurrence. Intermittency is primarily a factor at higher altitudes outside the surface layer,[8] but it can, to a lesser extent, also occur at lower altitudes. Although filtered white noise models, as noted by Panofsky and Dutton, produce the correct average results, they are incapable of simulating these low-probability events.

A possible alternative to spectral modeling is the so-called full simulation method (see Ref. 9, pp. 159-161). In this approach, the underlying Navier-Stokes equations that describe the dynamics of the turbulence are solved for quantities like temperature and pressure. Using Equation 2.8 or a similar expression, these parameters are converted to an index of refraction. The electromagnetic propagation can then be simulated using the parabolic equation. This approach was used by Rouseff et al.[21] to study the effects of oceanic microstructure on acoustic propagation over short ranges. Although the entire procedure was conceptually complete, it is likely to be impractical for large-scale atmospheric simulations. The inner and outer scales of turbulence differ by perhaps five orders of magnitude; to simulate the entire medium with the necessary resolution out to ranges on the order of tens of kilometers would be computationally prohibitive. The increased availability of super computing technology may make this approach more attractive in the future.

Wave propagation theories for random media have traditionally been formulated in terms of the spectrum of the medium. More recently, research has started to

---

[19] C. Macaskill and T. E. Ewart, "Computer Simulation of Two-Dimensional Random Wave Propagation," *IMA J. Appl. Math.* 33, 1-15 (1984).

[20] A. Papoulis, *Probability, Random Variables, and Stochastic Processes*, McGraw-Hill, New York (1984).

[21] D. Rouseff, K. B. Winters, and T. E. Ewart, "Reconstruction of Oceanic Microstructure by Tomography," *J. Geophys. Res.* **96**, 8823-8834 (1991).

focus on calculating the probability distribution of the field.[22,23] As these theories become more fully developed, it is possible that they could be used to assign probabilities of occurrence to abnormal events.

A new approach using fractals also has some potential for modeling turbulence. Kim and Jaggard[24] used fractals to simulate events exhibiting both turbulence-like spectra and intermittency. Jaggard[25] developed analytical solutions for optical propagation through a succession of fractal phase screens. Because of the close parallels between propagation through phase screens and what is actually implemented in a parabolic equation routine (see section 4.1), it seems likely that fractal phase screens could be used in TEMPER. It appears unlikely, however, that fractal phase screens could be generated using efficient numerical techniques like the FFT.

To summarize, spectral models are relatively easy to implement and have traditionally been used in conjunction with the parabolic equation method. Useful results have long been obtained in ocean acoustics applications. Spectral modeling can be a fruitful approach if the objective of a numerical study is to calculate the average fluctuations in the field caused by randomness. The method cannot, however, be used to simulate low-probability events.

---

[22]T. E. Ewart, "A Model of the Intensity Probability Distribution for Wave Propagation in Random Media," *J. Acoust. Soc. Am.* **86**, 1490-1498 (1989).

[23]E. Jakeman, "Scattering by Gamma-Distributed Phase Screens," *Waves in Random Media* **2**, 153-167 (1991).

[24]Y. Kim and D. L. Jaggard, "Band-Limited Fractal Model of Atmospheric Refractivity Fluctuation," *J. Opt. Soc. Am. A: Opt. Image Sci.* **5**, 475-481 (1988).

[25]D. L. Jaggard, "On Fractal Electrodynamics," in *Recent Advances in Electromagnetic Theory*, H. N. Kritikos and D. L. Jaggard (ed.), Springer-Verlag, New York (1991).

# 3. THEORETICAL SOLUTIONS FOR PROPAGATION THROUGH RANDOM MEDIA

Tractable analytical solutions for predicting the statistical properties of an electromagnetic wave propagating through a random medium are available only for certain idealized source configurations such as a plane wave or a point source. These solutions usually neglect both deterministic index of refraction profiles and the interaction of the field with any boundaries. To solve these more difficult problems, numerical techniques such as the parabolic equation method are necessary. For two important reasons, however, it is still crucial to consider the analytical solutions, despite their limited applicability. First, the solutions for the canonical problems provide a benchmark for testing numerical algorithms. Second, the analytical solutions provide insight as to how three-dimensional turbulent fluctuations should be modeled for inclusion in two-dimensional numerical simulations.

Fundamentally, TEMPER solves a two-dimensional wave propagation problem. This two-dimensional problem is interpreted as representing a cross-sectional slice of the true three-dimensional reality, which is reasonable for propagation through deterministic media that are varying in a scale very large compared to the wavelength. Random turbulent fluctuations, however, can vary on scales as small as a millimeter. Consequently, the relationship between the two- and three-dimensional problems is no longer clear. In section 3.4, this relationship is examined in detail for plane wave propagation. If the statistical quantity of interest is the second moment of the field, then the two-dimensional result accurately predicts the cross-sectional behavior of the true three-dimensional problem. Two-dimensional simulations cannot, however, accurately predict the true log-amplitude fluctuations except in the very far field.

## 3.1 STRONG AND WEAK SCATTERING THEORIES

First, neglect atmospheric ducting and sea surface interaction and consider the idealized problem of a wave propagating through a medium characterized by small random fluctuations in its index of refraction. After propagating a short distance, the wavefront will start to acquire small deviations from its expected value owing to the randomness. The total field can be interpreted as the original coherent wave front plus a small random incoherent component. At greater distances, the cumulative effect of the random scattering will produce fluctuations on the same order as the original signal. Finally, at still greater ranges, the random component completely dominates and the field is essentially incoherent.

The theoretical approach used to calculate the statistical properties of the propagating wave depends on the range of interest. At sufficiently short ranges, where the contribution due to randomness is small, weak scattering theory is applicable. Weak scattering theory uses either the Born or the Rytov approximation to model the propagating field within the medium. For forward propagation through smoothly fluctuating media, the Rytov approximation is generally regarded as superior. If the scattering is sufficiently weak, there is no practical difference between the two approximations. At longer ranges, where the incoherent component of the field is large, strong scattering theory is required. In

this approach, partial differential equations are derived to describe the first, second, and higher moments of the total field. Beyond the second moment, numerical techniques are generally necessary to solve the equations approximately; this is the subject of active research.

Microwave propagation through a random medium differs from the analogous optical and ocean acoustic scattering problems in that most practical problems can be modeled by weak scattering theory. Figure 3.1 shows the rough regions of validity of the alternate theoretical approaches for plane wave propagation through a strongly turbulent atmosphere. At optical frequencies, strong scattering theory is necessary beyond about 1 km. At a frequency of 10 GHz, however, weak scattering is valid to a height of roughly 1000 km. Consequently, weak scattering theory will be emphasized in this analysis. It can be shown that strong scattering theory produces expressions that are consistent with weak scattering predictions in the appropriate limiting cases and for the appropriate statistical quantities.

Weak scattering theory gives integral expressions for various statistics of the field in terms of the fluctuations of the medium. The approach used to solve the integrals depends on the frequency and range of interest, and also on the scale of the irregularities. As noted in section 2, turbulence is characterized by an inner scale $\ell_0$ and an outer scale $L_0$. Figure 3.1 shows the subregions of weak scattering for various values of $\ell_0$ and $L_0$. Consider a range $L$ and an illuminating wavelength $\lambda$. If $L << \ell_0^2 / \lambda$, the Rytov integral is approximated using geometric optics; for microwave frequencies, this region is of little practical interest. For ranges $\ell_0^2 / \lambda << L << L_0^2 / \lambda$, both the inner and outer scales can affect the propagation and the field is said to be in the diffraction (Fresnel) regime. (A note of caution is in order. The phrase "diffraction regime" is used here differently than in radar work, where it commonly refers to over-the-horizon propagation.[1]) Finally, for $L >> L_0^2 / \lambda$, the Rytov integral is well approximated using the far field or Fraunhofer approximation.

Let the field at point $\mathbf{r}$ after propagating from the source through randomness be given by $U(\mathbf{r}) = A(\mathbf{r}) \exp [(iP\mathbf{r})]$. Designate the field that would exist at the same point, coming from the same source but without randomness, as $U_0(\mathbf{r}) = A_0 \exp [iP_0(\mathbf{r})]$. As noted earlier, weak scattering theory gives expressions for various statistical quantities. Among these are the autocorrelation $B_\chi$ of the normalized log-amplitude of the field and the autocorrelation $B_P$ of the normalized phase:

$$B_\chi(\mathbf{r}_1, \mathbf{r}_2) = \langle \chi(\mathbf{r}_1) \chi(\mathbf{r}_2) \rangle \tag{3.1a}$$

$$B_P(\mathbf{r}_1, \mathbf{r}_2) = \langle P_1(\mathbf{r}_1) P_1(\mathbf{r}_2) \rangle, \tag{3.1b}$$

where the angle brackets indicate an ensemble average and

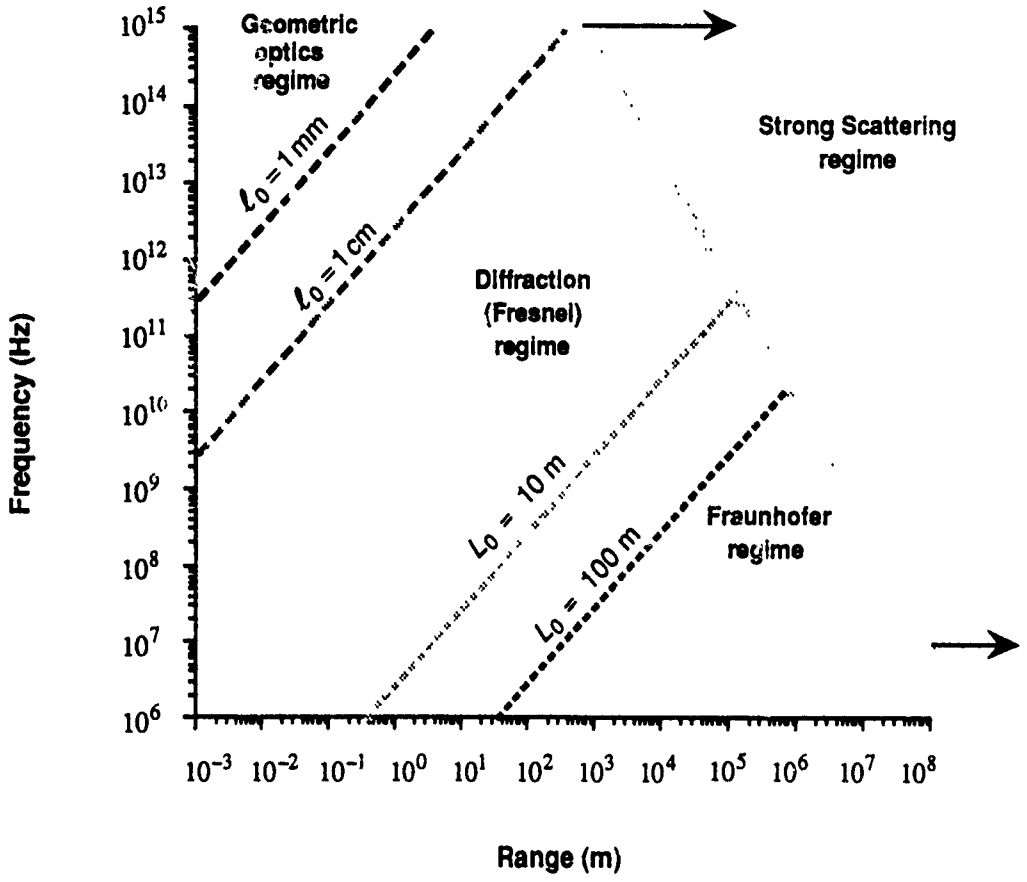


**Figure 3.1** Scattering regimes for a plane wave propagating through strong turbulence. The negatively sloping shaded line indicates the break between strong and weak scattering theories. Weak scattering, based on the Rytov approximation, is further divided into the geometric optics, the diffraction, and the Fraunhofer subregions. The broken lines between the weak scattering subregions depend on the inner scale $\ell_0$ and the outer scale $L_0$ of the turbulence. The line between strong and weak scattering is set where the variance of the field log-amplitude fluctuations equals 0.2 (see Eq. 3.9) and the structure constant $C_n$ for turbulence is set to $10^{-7}$.

$$\chi(\mathbf{r}) = \ln\left[A(\mathbf{r}) / A_0(\mathbf{r})\right] \tag{3.2a}$$

$$P_1(\mathbf{r}) = P(\mathbf{r}) - P_0(\mathbf{r}). \tag{3.2b}$$

The log-amplitude is frequently a quantity of interest for radar work. Since the phase is related to the travel time of the wave, the phase fluctuations are often the quantities of interest in ocean acoustics. The associated structure functions are given by

$$D_\chi(\mathbf{r}_1, \mathbf{r}_2) = \left\langle \left|\chi(\mathbf{r}_1) - \chi(\mathbf{r}_2)\right|^2 \right\rangle \tag{3.3a}$$

$$D_P(\mathbf{r}_1, \mathbf{r}_2) = \left\langle \left|P_1(\mathbf{r}_1) - P_1(\mathbf{r}_2)\right|^2 \right\rangle. \tag{3.3b}$$

Both the log-amplitude and the phase are quantities that are natural to calculate within the Rytov approximation. Within the Born approximation, it is natural to consider the scattered field

$$U_s(\mathbf{r}) = U(\mathbf{r}) - U_0(\mathbf{r}) \tag{3.4}$$

with the associated autocorrelation

$$B_s(\mathbf{r}_1, \mathbf{r}_2) = \left\langle U_s(\mathbf{r}_1) U_s^*(\mathbf{r}_2) \right\rangle. \tag{3.5}$$

Although the log-amplitude and phase are both real functions of position, the scattered field is complex. Note also that the mean incident field is subtracted from the total in Equation 3.4 to yield the scattered field. Hence for weak scattering the autocorrelation of the scattered field can be interpreted as the autocovariance of the total.

Strong scattering theory produces expressions for the statistical moments of the total complex field $U(\mathbf{r}) = A(\mathbf{r}) \exp[iP(\mathbf{r})]$. Much of the current research concentrates on solving for the fourth moment, which can be related to intensity scintillation. For comparison with weak scattering theory, however, the second moment of the field will be emphasized at range $L$, defined by

$$\Gamma(x = L; y_1, z_1; y_2, z_2) = \left\langle U(x = L, y_1, z_1) U^*(x = L, y_2, z_2) \right\rangle. \tag{3.5}$$

Particularly in optics, the second moment is called the mutual coherence function.

## 3.2 PLANE WAVE PROPAGATION

Consider the correlation of the field at points $\mathbf{r}_1$ and $\mathbf{r}_2$ at common range $x_1 = x_2 = L$. If the medium is statistically homogeneous, the field statistics will be a function of the difference coordinates $y_d = y_1 - y_2$ and $z_d = z_1 - z_2$. The integral expressions within the Rytov approximation are[26]

$$B_\chi(L, y_d, z_d) = \pi k^2 L \int_{-\infty}^{\infty} dk_y \int_{-\infty}^{\infty} dk_z S_n(0, k_y, k_z) \exp[-i(k_y y_d + k_z z_d)] f_\chi(\kappa), \tag{3.7a}$$

$$B_P(L, y_d, z_d) = \pi k^2 L \int_{-\infty}^{\infty} dk_y \int_{-\infty}^{\infty} dk_z S_n(0, k_y, k_z) \exp[-i(k_y y_d + k_z z_d)] f_P(\kappa), \tag{3.7b}$$

where $k = 2\pi/\lambda$ is the wave number, $\kappa^2 = k_y^2 + k_z^2$, and $S_n$ is the three-dimensional spectrum of the index of refraction. The functions $f_\chi$ and $f_P$ are called the spectral filter functions for the log-amplitude and phase, respectively, and are given by

$$f_\chi(\kappa) = 1 - \frac{\sin(\kappa^2 L/k)}{\kappa^2 L/k}, \tag{3.8a}$$

$$f_P(\kappa) = 1 + \frac{\sin(\kappa^2 L/k)}{\kappa^2 L/k}. \tag{3.8b}$$

If the medium is also isotropic, single integral expressions are available (see Ref. 4, p. 359).

For a turbulent medium within the Fresnel regime, $\ell_0^2 / \lambda << L << L_0^2 / \lambda$, the dominant contribution to the integration in Equation 3.7a comes from the inertial subrange of the Kolmogorov spectrum and $S_n = 0.033\kappa^{-11/3}$ can be used for all $\kappa$. Evaluating at $y_d = z_d = 0$ gives the variance of the log-amplitude (see Ref. 4, p. 370):

$$\sigma_\chi^2 \equiv B_\chi(L, y_d = z_d = 0) = 0.307 C_n^2 k^{7/6} L^{11/6}. \tag{3.9}$$

Equation 3.9 was used to define the transition between weak and strong scattering in Figure 3.1. Weak scattering theory can be used for $\sigma_\chi^2 < 0.2 - 0.5$. Within the Fresnel regime, Equation 3.7a can also be approximated for arbitrary correlation distance. The resulting expression is extremely cumbersome (see Ref. 4, p. 370).

The general expressions for the autocorrelations simplify considerably within the Fraunhofer regime. Except for very small $\kappa$, the spectral filter functions of

---

[26]S. M. Rytov, Y. A. Kravtsov, and V. I. Tatarskii, *Principles of Statistical Radiophysics*, Vol. 4, Springer-Verlag, New York (1989).

Equation 3.7 are both approximately equal to 1 for the significant part of the integration (see Ref. 4, p. 364, and Ref. 26, p. 57):

$$f_\chi \cong f_P \cong 1 \quad \text{(Fraunhofer regime)}. \tag{3.10}$$

Equation 3.7 can thus be approximated by

$$B_\chi \cong B_P \cong k^2 L \int_0^\infty B_n(x_d, y_d, z_d) dx_d, \tag{3.11}$$

where it has been assumed that the autocorrelation of the medium exists.

Approximating the spectral filters by a constant simplifies the resulting integral expressions for the log-amplitude and phase fluctuations. However, the approximate expressions are only marginally useful for propagation through turbulence. For example, consider a 3.3-GHz plane wave propagating through a turbulent medium with an outer scale of 100 m. The Fraunhofer criterion is met for ranges much greater than 110 km. For an outer scale of 10 m, the far field applies at ranges much greater than 1.1 km.

For the scattered field, the autocorrelation is given by

$$B_s(L, y_d, z_d) = \pi k^2 L \int_{-\infty}^{\infty} dk_y \int_{-\infty}^{\infty} dk_z S_n(0, k_y, k_z) \exp[-i(k_y y_d + k_z z_d)] f_s(\kappa), \tag{3.12a}$$

where $f_s$, the spectral filter for the scattered field, can be written in terms of the spectral filters for the log-amplitude and the phase:

$$f_s = f_\chi + f_P = 2. \tag{3.12b}$$

Note that the spectral filter for the scattered field is constant for arbitrary range. This is in contrast to the log-amplitude and the phase, where the the associated spectral filters are approximately constant only at very distant ranges. Assuming the autocorrelation of the medium exists, Equation 3.12a can be rewritten as

$$B_s(L, y_d, z_d) = 2k^2 L \int_0^\infty B_n(x_d, y_d, z_d) dx_d. \tag{3.13}$$

Equation 3.13 will be used in section 4 to calculate the expected solutions to which numerical simulations will be compared.

For strong scattering theory, the mutual coherence function is given by (see Ref. 4, p. 414, and Ref. 6, p. 31)

$$|\Gamma| = C_s \exp\left[-\frac{1}{2} D(y_d, z_d)\right], \tag{3.14}$$

where $C_s = 1$ for a plane wave. $D(y_d,z_d)$ is the wave structure function and is related to the log-amplitude and phase structure functions used in Rytov theory (Eq. 3.2) by

$$D(y_d, z_d) = D_\chi(y_d, z_d) + D_P(y_d, z_d). \tag{3.15}$$

By appropriate expansions, it can be shown than Equation 3.14 is consistent with Equation 3.13 when $|D| << 1$.

Equation 3.14 is a typical strong scattering result. When the random fluctuations in the index of refraction are assumed to occur about some deterministic mean profile, the wave structure function can be written in terms of path integrals through the medium.[27,28] Evaluation of these path integrals is the subject of current research in the scattering community.

## 3.3 POINT SOURCE PROPAGATION

Point source illumination is another important geometry for which closed form expressions are available. Because the numerical simulations in section 4 emphasize plane waves, only the primary point source results are summarized here. (For greater detail, see Refs. 4 and 7.) In weak scattering, the derivation begins by making the Rytov approximation to the scattering integral. A paraxial approximation is then made for both the incident field and the free space Green's function. The variance of the normalized log-amplitude fluctuations for a turbulent medium is given by (Ref. 4, p. 379)

$$\sigma_\chi^2 = 0.124 C_n^2 k^{7/6} L^{11/6}, \tag{3.16}$$

which can be compared to the analogous plane wave result in Equation 3.9.

For strong scattering, the mutual coherence is again given by Equation 3.14 with $C_s = L^{-2}$.

## 3.4 RELATIONSHIP BETWEEN TWO- AND THREE-DIMENSIONAL PROBLEMS

The parabolic equation/split-step algorithm as implemented in TEMPER solves a two-dimensional propagation problem. The results are interpreted as representing propagation in a vertical cross-section of the true three-dimensional geometry.

---

[27]S. M. Flatté, R. Dashen, W. H. Munk, K. M. Watson, and F. Zachariasen, *Sound Transmission Through a Fluctuating Ocean*, Cambridge University Press, New York (1979).

[28]S. M. Flatté, "Wave Propagation through Random Media: Contributions from Ocean Acoustics," *Proc IEEE* **71**, 1267-1294 (1983).

This is reasonable for propagation through a deterministic medium, since it is typically fluctuating on a scale that is very large compared to the wavelength $\lambda$ and out-of-plane scatter is small. It is not obvious, however, that this approximation remains valid when random turbulent fluctuations are included. As noted in section 2.1, the inner scale of turbulence can be as little as a millimeter. Consequently, a turbulent medium will contain fluctuations that are small compared to $\lambda$ at microwave frequencies. In this section, theoretical solutions for the two-dimensional problem that is actually simulated by TEMPER are considered. The conditions under which the two-dimensional solutions might be legitimately interpreted as representing a cross-section of the three-dimensional problem are given.

Consider the statistics of the propagating field evaluated along a vertical line. The weak scattering plane wave results given in Equations 3.7 and 3.12 can be written in a compact notation as

$$B_Q(L,y_d,z_d) = \pi k^2 L \int_{-\infty}^{\infty} dk_y \int_{-\infty}^{\infty} dk_z S_n(0,k_y,k_z)\, \exp[-i(k_y y_d + k_z z_d)] f_Q(\kappa)\,, \tag{3.17}$$

where $Q$ can be $\chi$, $P$, or $s$ to represent the log-amplitude, the phase, or the scattered field, respectively. Following the derivation of Ishimaru,[4] it can be shown that the same statistical quantities in the two-dimensional problem are given by

$$B_Q^{(2)}(x = L, z_d) = \pi k^2 L \int_{-\infty}^{\infty} dk_z S_n^{(2)}(k_x = 0, k_z)\, \exp(+ik_z z_d) f_Q(k_z). \tag{3.18}$$

Comparing the two expressions, we see that Equation 3.17 reduces to Equation 3.18 for any special filter function $f_Q$ if the three-dimensional spectrum is of the form

$$S_n(k_x,k_y,k_z) = S_n^{(2)}(k_x,k_z)\delta(k_y). \tag{3.19}$$

Equation 3.19 states the trivial result that the three-dimensional problem reduces to two dimensions if there is no variation in the transverse coordinate; this clearly is not the case for atmospheric turbulence. As an alternative, we must design the two-dimensional spectrum to mimic the three-dimensional fluctuations. The way in which this is done will depend on the spectral filter function $f_Q$. For the scattered field, $Q = s$ and the spectral filter is constant. Under these circumstances, Equations 3.17 and 3.18 are equivalent at $y_d = 0$ if

$$S_n^{(2)}(k_x,k_z) = \int_{-\infty}^{\infty} dk_y S_n(k_x,k_y,k_z). \tag{3.20}$$

Taking the inverse transform of Equation 3.20 relates the two autocorrelations

$$B_n^{(2)}(x_d, z_d) = B_n(x_d, y_d = 0, z_d). \tag{3.21}$$

Hence the two-dimensional random process is simply a cross-section of the three-dimensional process evaluated along a vertical plane.

Equation 3.21 is a significant result; it implies that meaningful results can be obtained from two-dimensional simulations. Further, it gives a simple relationship between the three-dimensional statistics of the medium that are measured and the two-dimensional statistics that will be used in the simulations. This cross-sectional notion has been routinely used in numerical studies of strong scattering phenomena.[19] This analysis suggests that this assumption is also true for weak scattering provided the statistical quantity of interest is the fluctuations of the scattered field.

Mathematically, this dimensional simplification was possible because the spectral filter for the scattered field is a constant. Except in the far field, however, the spectral filter functions for the log-amplitude and the phase fluctuations are not constant and the simple partitioning used above is not valid. At ranges in the Fresnel regime, the oscillatory part of the spectral filters in Equation 3.8 contributes to the autocorrelation integrals. At distant ranges in the Fraunhofer regime, the oscillatory contribution can be neglected, the spectral filters approximated by constants (Eq. 3.10), and the cross-sectional assumption again becomes reasonable.

To summarize, if the statistical quantity of interest is the autocorrelation of the scattered field, then it is valid to simulate a cross-section of the three-dimensional medium. The result holds for arbitrary range. In calculations of the log-amplitude fluctuations or the phase fluctuations, however, the cross-sectional assumption is approximately correct only in the far field.

To quantify the results of the preceding section, consider a medium characterized by an isotropic Gaussian autocorrelation:

$$B_n(x_d, y_d, z_d) = \sigma_n^2 \exp\left[-(x_d^2 + y_d^2 + z_d^2) / \ell_0^2\right]. \tag{3.22}$$

While the Gaussian spectrum does not represent any true medium, it is mathematically more convenient to manipulate than the von Karman spectrum and is adequate for this example. An expression for the variance of the log-amplitude is given by Ref. 26 (p. 77). Converting to the notation used in this paper,

$$\sigma_\chi^2 = \frac{1}{2}\sqrt{\pi}\,\sigma_n^2 k^2 L \ell_0 \left[1 - D^{-1}\tan^{-1}(D)\right], \tag{3.23}$$

where $D = kL / (k\ell_0 / 2)^2$. The first term inside the square brackets in Equation 3.23 is from the constant part of the spectral filter and is the far field (large $D$) result. The second term, $D^{-1}\tan^{-1}(D)$, is due to the oscillatory part of the spectral

filter; it can be interpreted as the Fresnel (diffraction) correction. For ranges $L >> \ell_0^2 / \lambda$, that is, $D >> 1$, this term falls like $D^{-1}$.

A similar derivation is possible for a two-dimensional geometry. Evaluating Equation 3.22 at $y_d = 0$ yields the two-dimensional autocorrelation. Taking the Fourier transform yields the spectrum. The spectrum along with the log-amplitude spectral filter (Eq. 3.8a) are substituted into Equation 3.18. With $z_d = 0$ and a suitable change of variables, the resulting integral can be evaluated,[29] yielding

$$\sigma_\chi^2 = \frac{1}{2}\sqrt{\pi}\,\sigma_n^2 k^2 L \ell_0 \left\{1 - 2D^{-1}(1+D^2)^{1/4} \sin\left[\frac{1}{2}\tan^{-1}(D)\right]\right\}. \qquad (3.24)$$

As expected, the first term, that is, the far field Fraunhofer result, is equivalent in the two expressions. Note, however, that the second term falls like $D^{-1/2}$ for $D >> 1$ This is a significantly slower falloff than is observed for the three-dimensional case; the two-dimensional case reaches the far field more slowly.

As a numerical example, consider the following typical values:

| | |
|---|---|
| Frequency | 3.3 GHz ($k$ = 69.12 m$^{-1}$) |
| Range | 4.9 nautical miles ($L$ = 9075 m) |
| Correlation length | 10 feet ($\ell_0$ = 3.04 m) |
| Variance of medium | $\sigma_n^2 = 10^{-12}$ |
| D | $= (k L) / (k \ell_0/2)^2 = 56.8$ |

Substituting into Equations 3.23 and 3.24 yields

Three-dimensions:

$$\sigma_\chi^2 = \frac{1}{2}\sqrt{\pi}\,\sigma_n^2 k^2 L \ell_0 (1 - 0.027) = 11.36 \times 10^{-5},$$

Two-dimensions:

$$\sigma_\chi^2 = \frac{1}{2}\sqrt{\pi}\,\sigma_n^2 k^2 L \ell_0 (1 - 0.186) = 9.51 \times 10^{-5}.$$

While the correction term in the three-dimensional case makes only a 2.7% contribution, the corresponding term in two-dimensions contributes 18.6%. This example suggests that the use of two-dimensional simulations to calculate the three-dimensional log-amplitude fluctuations must be viewed skeptically.

---

[29] I. S. Gradshteyn and I. M. Ryzhick, *Tables of Integrals, Series and Products*, Academic Press, Orlando, Fla., p. 490 (1980).

# 4. MODELING TURBULENT FLUCTUATIONS IN TEMPER

Having developed the necessary background theory, we are now ready to consider proposed methods for including turbulent refractive index fluctuation in TEMPER.

As shown by Ko et al.,[30] derivation of the electromagnetic parabolic equation usually begins by assuming a spherical coordinate system with the origin at the center of an Earth of radius $a_e$ and a vertical electric (or magnetic) dipole source located at $r = a_e + h$ and $\theta = 0$. In deriving the time-independent wave equation, all derivatives with respect to the $\phi$ coordinate are ignored. This is justified through the rotational symmetry of the source and by assuming the medium is rotationally symmetric about the source point. The problem is reduced to two dimensions and through a conformal transformation it is written in pseudo-rectangular coordinates.[2] Some form of the parabolic approximation is then made to admit a marching solution through the Fourier split-step method. Using this two-dimensional assumption as a starting point, a method for including random fluctuations is developed.

## 4.1 INCLUDING RANDOMNESS IN TEMPER

TEMPER solves the two-dimensional parabolic equation with height $z$ and range $x$. The field $u$ at range $x$ is propagated to $x + \delta x$ by the algorithm[1]

$$u(x+\delta x, z) = \frac{1}{2\pi} \exp[ik\phi(z)] \int_{-\infty}^{\infty} dp \exp(ipz) \exp\left[\frac{-ip^2 \delta x}{2k}\right] \cdot \int_{-\infty}^{\infty} dz' u(x,z') \exp(-ipz'), \tag{4.1}$$

where $k = 2\pi/\lambda$ is the free space wave number and $\exp[ik\phi(z)]$ is the transmittance function with

$$\phi(z) = \frac{1}{2} \int_{x}^{x+\delta x} dx' \left[n^2(x',z) - 1\right] + z\delta x / a_e, \tag{4.2}$$

where $n$ is the index of refraction.

The procedure can be summarized as follows: take the Fourier transform with respect to height of the given initial field distribution, multiply by a propagation filter, inverse transform, and finally multiply by a transmittance function that represents the effects of the medium between $x$ and $x + \delta x$. The split-step algorithm separates the propagation effects from the effects of the medium; the field is propagated a distance $\delta x$ as if through free space and then *a posteriori* multiplied by the transmittance that modulates the phase of the field to account for

---

[30] H. W. Ko, J. W. Sari, and J. P. Skura, "Anomalous Microwave Propagation through Atmospheric Ducts," *Johns Hopkins APL Tech Dig.* 4, 12-26 (1983)

the integrated effects of the medium. In analogy with optics, the transmittance function is usually called a phase screen.

The index of refraction includes a deterministic, height-dependent mean profile $<n(z)>$ and a small randomly fluctuation part $n_f(x,z)$:

$$n(x,z) = 1 + < n(z) > + n_f(x,z). \tag{4.3}$$

The profile may be weakly range dependent, but for simplicity is assumed here to be independent of $x$ over the step size. Assuming $|<n> + n_f| << 1$ and neglecting second-order terms yields

$$\phi(z) = [< n > + z / a_e]\delta x + \phi_t(z), \tag{4.4a}$$

where $\phi_t$ represents the integrated random refractive index fluctuations,

$$\phi_t(z) = \int_x^{x+\delta x} dx' n_f(x',z). \tag{4.4b}$$

The objective is to generate random realizations of $\phi_t$ consistent with the assumed statistics of $n_f$. For this two-dimensional problem, the random part of the refractive index is modeled as a zero mean, statistically homogeneous process with an autocorrelation function $B_n^{(2)}(x_d, z_d)$. It follows from Equation 4.4b that $\phi_t$ is zero mean, with autocorrelation given by

$$\left\langle \phi_t(z_1)\phi_t(z_2) \right\rangle = \int_x^{x+\delta x} dx_1 \int_x^{x+\delta x} dx_2 B_n^{(2)}(x_1 - x_2, z_1 - z_2). \tag{4.5}$$

Changing the integration variables to $x_S = (x_1 + x_2)/2$ and $x_d = (x_1 - x_2)$, and assuming that the step size $\delta x$ is large compared to the correlation length of the medium, yields approximately

$$\left\langle \phi_t(z_1)\phi_t(z_2) \right\rangle \equiv \delta x \int_{-\infty}^{\infty} dx_d B_n^{(2)}(x_d, z_d) \equiv B_t(z_d). \tag{4.6}$$

The quantity $B_t$ is called the transverse autocorrelation and plays an important role in strong scattering theory.[6] With an eye toward eventual implementation in Appendix A using the fast Fourier transform, we define the associated transverse spectrum by

$$S_t(k_z) = \int_{-\infty}^{\infty} dz_d B_t(z_d) \exp(-ik_z z_d). \tag{4.7}$$

For consistency with the three-dimensional spectra used in section 2, the two-dimensional spectrum of the medium is defined by

$$S_n^{(2)}(k_x,k_z)=\left(\frac{1}{2\pi}\right)^2\int_{-\infty}^{\infty}dx_d\int_{-\infty}^{\infty}dz_d B_n^{(2)}(x_d,z_d)\exp[-i(k_x x_d+k_z z_d)]. \tag{4.8}$$

Combining Equations 4.6–4.8 relates the transverse spectrum to the two-dimensional spectrum of the medium

$$S_t(k_z)=(2\pi)^2\,\delta x\,S_n^{(2)}(k_x=0,k_z). \tag{4.9}$$

Realizations of $\phi_t$ consistent with this transverse spectrum can be generated using the algorithm in Appendix A. These fluctuations can then be included in the marching algorithm of Equation 4.1 to simulate propagation through a single realization of a random medium. The statistical properties of the propagating field for any given realization can be estimated. As part of a Monte Carlo procedure, the simulation can be repeated for many independent realizations. By averaging the estimates, an overall estimate of the true ensemble characteristics is obtained.

One of the central assumptions of this derivation is that the step size $\delta x$ is large compared to the outer scale of the medium $L_0$. With this assumption, the phase screens at adjacent range steps are essentially uncorrelated and can be generated independently. If $\delta x < L_0$, then the individual screens are correlated and the medium must be generated using a two-dimensional FFT routine. Spivak[31] has shown that if the objective of a numerical study is to predict the correct ensemble statistics, then uncorrelated phase screens are adequate. Correlated screens are necessary if the objective is to mimic the fine detail that would truly exist in individual realizations. Correlated screens were also used by Rouseff and Porter[32] to test stochastic inverse scattering algorithms. Since the generation of correlated phase screens is much more computationally expensive, and since using filtered white noise to model turbulence is at best valid only in an ensemble sense anyway (section 2.5), uncorrelated screens will be used in this study.

The basic split-step algorithm of Equation 4.1 can be extended to three dimensions. The one-dimensional forward and inverse transforms are replaced by two-dimensional transforms along the transverse $y$-$z$ plane. The dimensionality of the phase screens is also increased. This approach was used by Martin and Flatté[33] to model optical propagation through turbulence. Unfortunately, adding the extra dimension makes the problem very computationally intensive: Martin and Flatté required a Cray super computer to implement their algorithm. As computer

---

[31]M. Spivack, "Accuracy of the Moments from Simulation of Waves in Random Media," *J. Opt Soc Am A* 7, 790-793 (1990).

[32]D. Rouseff and R. P. Porter, "Diffraction Tomography and the Stochastic Inverse Scattering Problem," *J Acoust Soc. Am.* **89**, 1599-1605 (1991)

[33]J. M. Martin and S. M Flatté, "Intensity Images and Statistics from Numerical Simulation of Wave Propagation in 3-D Random Media," *Appl Opt.* **27**, 2111-2127 (1988)

technology improves, full three-dimensional simulations may become practical for desk-top calculations. In the meantime, we are left with two-dimensional numerical models that attempt to predict three-dimensional phenomena.

The relationship between the two- and three-dimensional problems was discussed in section 3.4. If the quantity of interest is the scattered field, then at least for plane wave propagation it suffices to simulate a two-dimensional cross-section of the true three-dimensional medium. If the statistical quantity of interest is the log-amplitude or phase fluctuations of the field, then other strategies for simulating the medium must be developed. For simplicity, this preliminary numerical study will concentrate on calculating the second moment. The two- and three-dimensional spectra for the medium are related by Equation 3.20:

$$S_n^{(2)}(k_x,k_z)=\int_{-\infty}^{\infty} dk_y S_n(k_x,k_y,k_z)\,.$$

Combining Equations 3.20 and 4.9 relates the one-dimensional transverse spectrum used in parabolic equation simulations to the three-dimensional spectrum of the medium:

$$S_t(k_z)=(2\pi)^2\,\delta x\int_{-\infty}^{\infty} dk_y S_n(k_x=0,k_y,k_z). \qquad (4.10)$$

## 4.2 NUMERICAL EXAMPLE: PROPAGATION THROUGH A GAUSSIAN SPECTRUM

As a numerical example, we consider plane wave propagation through a medium described by a Gaussian spectrum. Although the Gaussian spectrum does not describe an actual medium, its properties lead to both a simple expression for the transverse spectrum and relatively rapid convergence in the Monte Carlo simulations.

The autocorrelation for an isotropic Gaussian correlated medium is given by Equation 3.22. The corresponding three-dimensional spectrum is easily calculated and substituted into Equation 4.10 to yield the transverse spectrum.

In the simulations, a 3.3-GHz plane wave is assumed, with the same set of parameters as used in section 3.4. The medium, 9075 m in extent, was represented by forty-nine equally spaced phase screens. In the vertical, a sampling interval of 0.2381 m was used with 1024 points.

The FFT routine of Press et al.[34] was used to implement the split-step algorithm of Equation 4.1. The random number generator RAN1 developed by Press et al. was used in the random phase model of Appendix A to produce the phase screens. The autocorrelation of the log-amplitude, the phase, and the scattered field of each realization was estimated using a standard unbiased estimator.[35] The procedure was repeated for 250 independent realizations; the

---

[34]W. H. Press, B. P. Flannery, S. A. Teukolsky, and W. T. Vetterling, *Numerical Recipes*, Cambridge University Press, Cambridge, England (1986).

[35]A. V. Oppenheim and R. V. Schafer, *Digital Signal Processing*, Prentice-Hall, Englewood Cliffs, N. J. (1975).

resulting averaged estimates and the theoretical prediction are plotted in Figure 4.1. The autocorrelation of the scattered field displays excellent agreement with the theoretical result calculated via Equation 3.13. At zero lag, the observed variance of the log-amplitude fluctuation is $9.56 \times 10^{-5}$, which is in good agreement with the predicted result ($9.51 \times 10^{-5}$) in section 3.4.

As expected, the two-dimensional numerical algorithm accurately predicts the vertical autocorrelation of the three-dimensional scattered field, but is unable to produce the desired log-amplitude fluctuations.

## 4.3 HOMOGENEOUS ISOTROPIC TURBULENCE

Within the constraints discussed in section 4.1, Equation 4.10 is valid for any three-dimensional homogeneous spectrum. The numerical example in section 3.2 used a Gaussian spectrum. One of the attractive features of this spectrum is that it is separable; the three-dimensional spectrum can be written as the product of three one-dimensional spectra. This simplifies the calculation of the transverse spectrum. Spectral models for internal waves and fine structure in the ocean are also separable.[36] Homogeneous isotropic turbulence is unfortunately not separable, and the resulting transverse spectrum must be expressed in terms of special functions. In this section, we calculate the transverse spectrum and associated autocorrelation function for homogeneous isotropic turbulence.

The von Karman spectrum is used to describe the three-dimensional index of refraction fluctuations. Substituting Equation 2.5 into Equation 4.10 yields

$$S_t(k_z) = 0.066(2\pi)^2 \delta x C_n^2 \exp(-k_z^2 / K_m^2) \int_0^\infty dk_y \frac{\exp(-k_y^2/K_m^2)}{(k_z^2+k_y^2+L_0^{-2})^{11/6}}. \quad (4.11)$$

After some manipulation, the integral in Equation 4.11 can be expressed exactly in terms of the confluent hypergeometric function $\psi$:[37]

$$S_t(k_z) = \frac{0.033(2\pi)^2}{(k_z^2 + L_0^{-2})^{4/3}} \delta x C_n^2 \pi^{1/2} \exp(-k_z^2/K_m^2) \psi\left[\frac{1}{2}; -\frac{1}{3}; K_m^{-2}(k_z^2 + L_0^{-2})\right]. \quad (4.12)$$

Equation 4.12 can be simplified in the inertial subrange. For spatial frequencies $\kappa$ in the inertial subrange and below, $K_m^{-2} k_z^2 << 1$. Hence the exponential can be set to 1 and $\psi$ can be replaced by its small argument approximation,

$$S_t(k_z) \equiv \frac{0.033(2\pi)^2}{(k_z^2 + L_0^{-2})^{4/3}} \delta x C_n^2 \pi^{1/2} \frac{\Gamma(4/3)}{\Gamma(11/6)}, \quad (4.13)$$

---

[36] T. E. Ewart and S. A. Reynolds, "Experimental Ocean Acoustic Field Moments versus Predictions," in *Ocean Variability and Acoustic Propagation*, J. Potter and A. Warn-Varnas (ed.), Kluwer Academic Publishers, Boston, Mass., pp. 23-40 (1991).

[37] M. Abramowitz and I. M. Stegun, *Handbook of Mathematical Functions*, National Bureau of Standards, Washington, D. C. (1965).

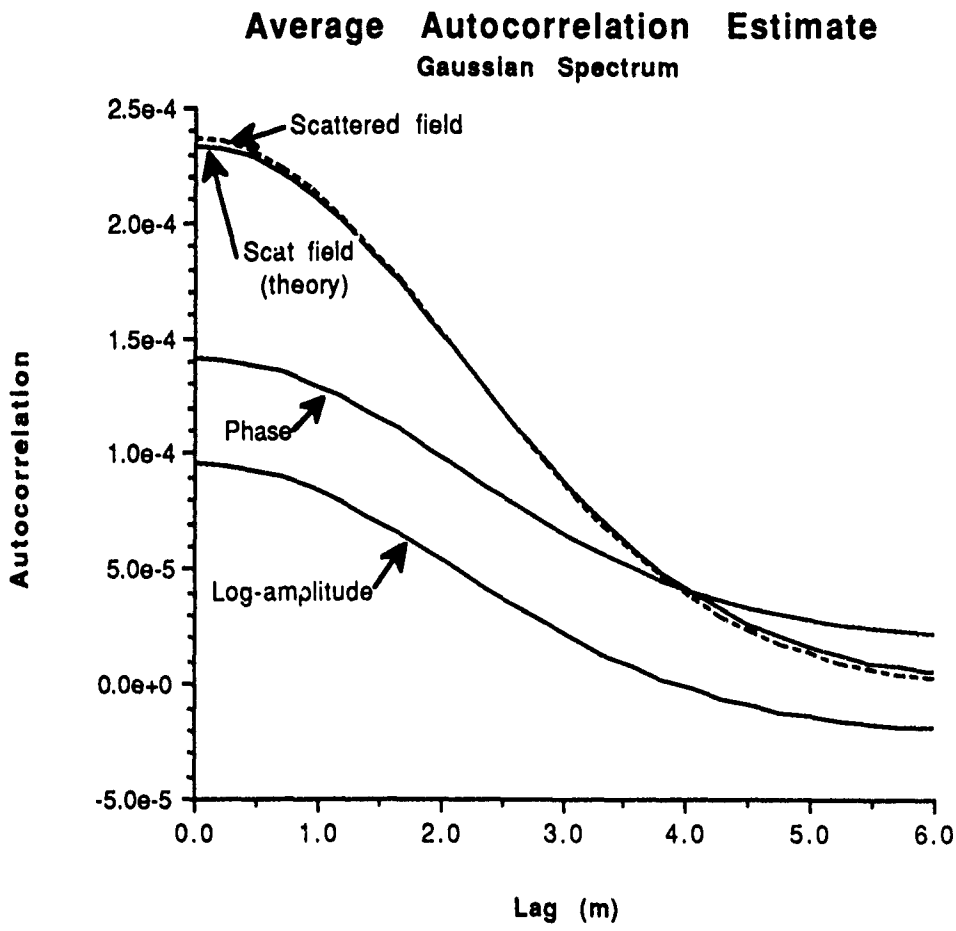


**Figure 4.1** Autocorrelations of field that has propagated through a medium with a Gaussian spectrum. Medium of variance $10^{-12}$ and correlation length 3.04 m are probed by 3.3-GHz plane wave. Theoretical scattered field autocorrelation is compared to numerical result. Phase and log-amplitude autocorrelations are also shown. Statistics are based on an ensemble average over 250 realizations. Each realization had forty-nine equally spaced phase screens of 1024 points and a vertical sampling interval of 0.2381 m. Read 2.5e-4 as $2.5 \times 10^{-4}$.

where $\Gamma$ is the gamma function. For parabolic equation simulations, the maximum spatial frequency of interest is determined by the wavelength $\lambda$ of the illuminating wave. Since typically for microwaves $\lambda > \ell_0$, the maximum frequency divided by $K_m$ will be much less than 1, and Equation 4.13 can be used for all spatial frequencies in parabolic simulations. For spatial frequencies in the inertial subrange, we observe that $S_t$ is proportional to $k_z^{-8/3}$.

Corresponding to the forward transform in Equation 4.7, the transverse autocorrelation function is given by the inverse transform

$$B_t(z_d) = \frac{1}{2\pi} \int_{-\infty}^{\infty} dk_z S_t(k_z) \exp(ik_z z_d). \tag{4.14}$$

Substituting the approximate transverse spectrum of Equation 4.13, the integral can be expressed in terms of a modified Bessel function,[38]

$$B_t(z_d) = \frac{0.033(2\pi)^2}{\Gamma(11/6)} \delta x C_n^2 \left(\frac{z_d L_0}{2}\right)^{5/6} K_{5/6}(z_d / L_0). \tag{4.15}$$

Using Equation 2.7, the transverse autocorrelation can also be written in terms of the variance of the index of refraction $< n_f^2 >$ as

$$B_t(z_d) = 2.647 \delta x \left\langle n_f^2 \right\rangle L_0 \left(\frac{z_d}{2L_0}\right)^{5/6} K_{5/6}(z_d / L_0), \tag{4.16}$$

where we have evaluated the gamma function. Equation 4.16 will be used as "truth" for the numerical simulations. This factorization is convenient for evaluating by a series expansion.

We note that Equation 4.16 is independent of the turbulent inner scale $\ell_0$. For microwaves, $\lambda >> \ell_0$ and the probing wave does not "see" the very small scale fluctuations. This is another case where the microwave problem differs from analogous propagation problems in optics.

As $z_d \to 0$, the small argument expansion of the modified Bessel function can be used to yield the variance of the transverse process:

$$B_t(0) = 1.494 \delta x \left\langle n_f^2 \right\rangle L_0. \tag{4.17}$$

The transverse variance is proportional to the variance of the medium and to the outer scale of the turbulence $L_0$.

Individual realizations of $\phi_t$ were generated using the transverse spectrum of Equation 4.13 and the algorithm in Appendix A. Figure 4.2 shows a 1024-point

---

[38]K. H. Craig and M. F. Levy, "Parabolic Equation Modelling of the Effects of Multipath and Ducting on Radar Systems," *IEE Proc. F* **138**, 153-162 (1991).

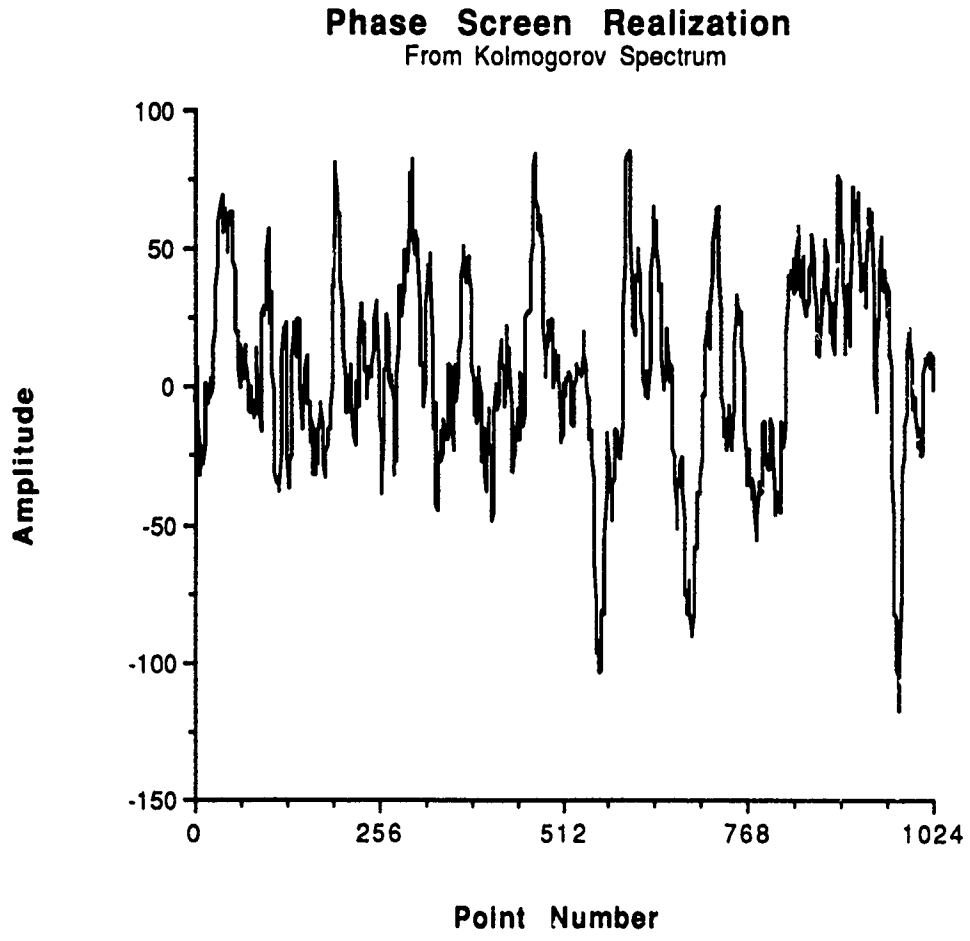


**Figure 4.2** Realization of $\phi_l$. Based on transverse spectrum in Equation 4.13 with $L_0$= 10 m. Step size is equal to 100 m. Unit variance and sampling.

realization with $L_0$ = 10 m, step size $\delta x$ = 100 m, and unit variance $< n_f^2 >$. Figure 4.3 shows an example where the outer scale has been increased to 100 m. This example vividly exhibits both the large- and small-scale fluctuations characteristic of power-law spectra. For comparison, Figure 4.3 also shows a realization generated using the same set of random numbers and the same outer scale but with a Gaussian spectrum, as was used in section 4.2. In contrast to a turbulent process that has both an inner and outer scale, a Gaussian spectrum is characterized by a single correlation length. As a result, the realization exhibits little of the detailed structure present in turbulence example.

Five hundred realizations of the process with $L_0$ = 10 m were generated. The autocorrelation of each was estimated using a standard unbiased estimator (see Ref. 35, p. 539). The estimates were then averaged across the ensemble and compared to the theoretical expression in Equation 4.21. The agreement is excellent and is shown in Figure 4.4. The study was repeated with the outer scale increased to 100 m. The average of 5000 estimates are compared to theory in Figure 4.5 with similar results. When the correlation length was increased, it was necessary to increase the number of realizations to get good agreement.

Realizations of the turbulent process with $L_0$ = 10 m were used in a propagation study. Aside from the different spectrum and outer scale, the remaining parameters are unchanged from the numerical example in section 4.2. Two hundred fifty independent simulations were used to estimate the ensemble statistics of the field. Figure 4.6 compares the predicted autocorrelation of the scattered field to three-dimensional theory. The agreement is excellent, particularly at short lags. Beyond the correlation length of the medium, the error becomes more noticeable. This is to be expected, since less information is available at large lags to make the estimates. To improve the agreement, the averaging could be conducted over more realizations. But since the validity of the turbulence model itself becomes questionable beyond the correlation length (section 2), it is probably not worth the effort.

Also shown in Figure 4.6 are the estimated log-amplitude and phase autocorrelation. Since the two curves differ significantly, we are clearly not in the two-dimensional Fraunhofer regime. At zero lag, the simulations give the log-amplitude variance to be $1.02 \times 10^{-4}$. The theoretical value calculated by Equation 3.9 is $3.19 \times 10^{-4}$. This example again illustrates that while the cross-sectional model produces good results for the moments of the field, it fails to calculate the log-amplitude fluctuations.

## 4.4 SURFACE LAYER TURBULENCE

The procedure for generating random realizations must be modified in the atmospheric surface layer. Sections 2.3 and 2.4 showed that at low altitudes both the structure constant $C_n^2$ and the outer scale $L_0$ must be treated as height-dependent variables. The only study known to model electromagnetic propagation through surface layer turbulence using the parabolic equation was conducted by Levy and Craig.[3,38] In this section, the algorithm used by Levy and Craig is critiqued, and it is suggested that they used an incorrect power law spectrum in their simulations. Possible modifications to existing meteorological models for surface layer turbulence are then considered to produce expressions compatible with our simula-

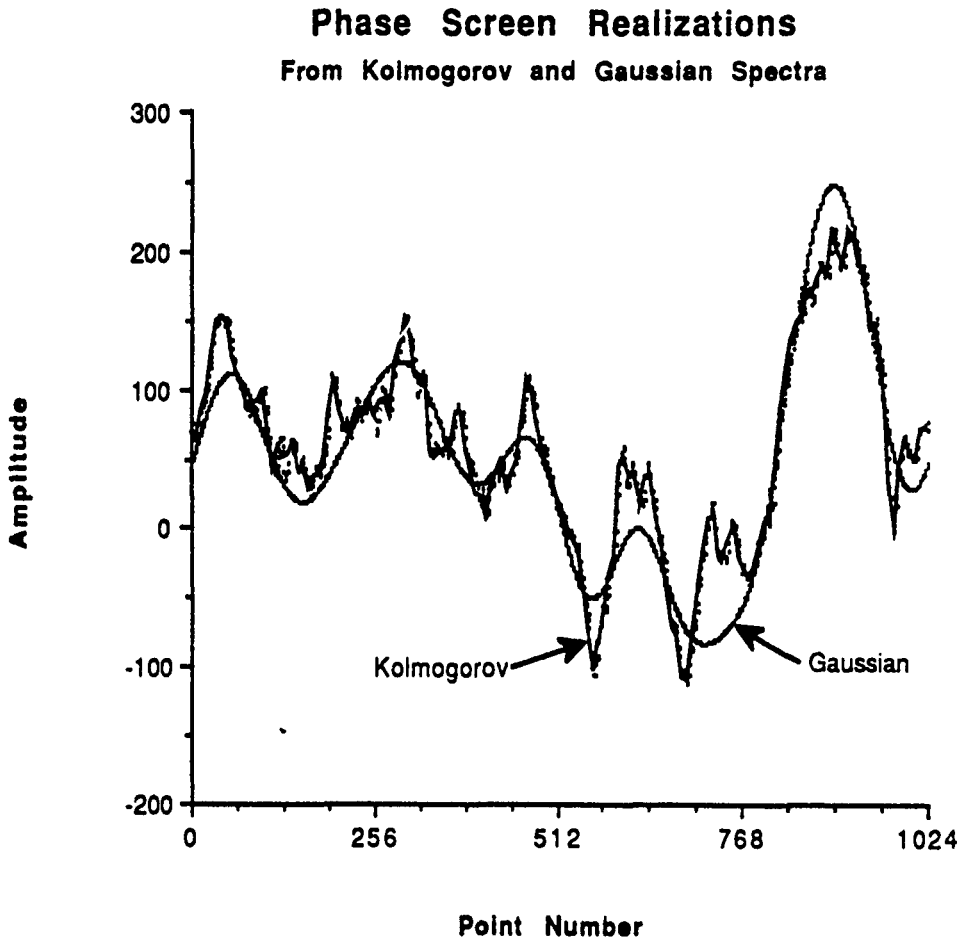


**Figure 4.3** Realization of $\phi_t$. Same as Figure 4.2 except with outer scale increased to 100 m. For comparison, realization of a process with the same outer scale but with a Gaussian spectrum is also shown. Step size is equal to 100 m. Unit variance and sampling.

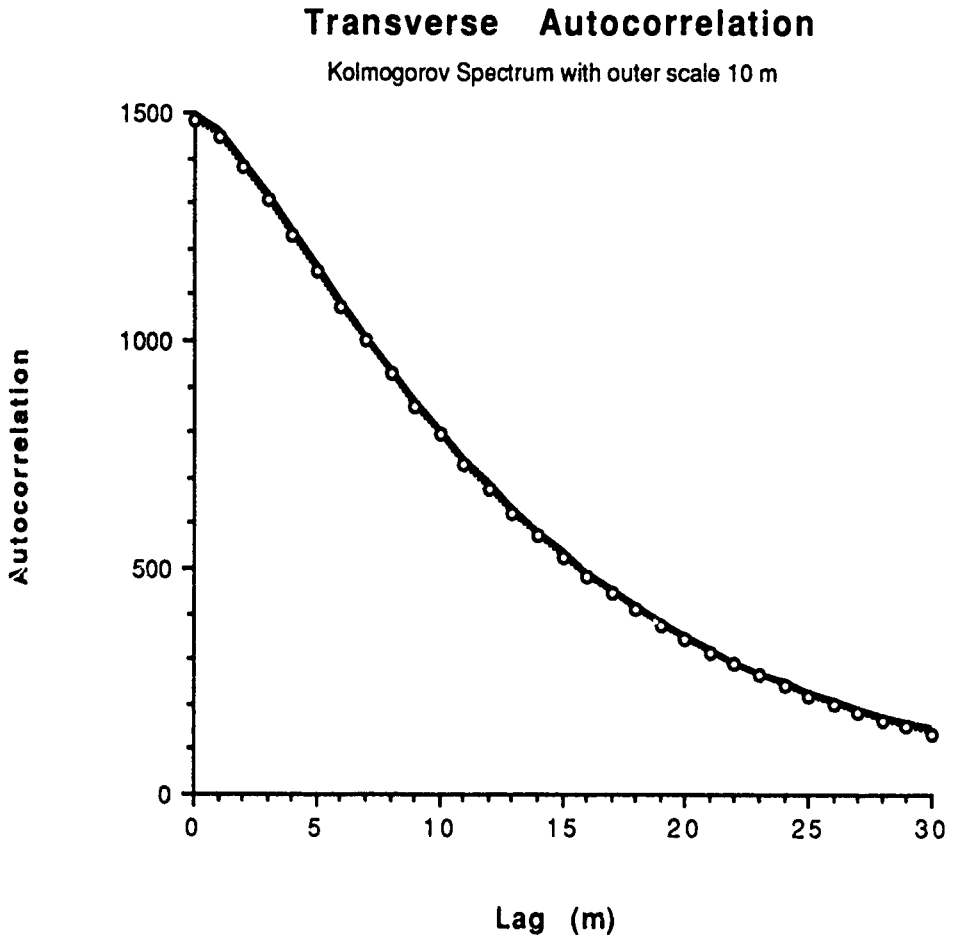


**Figure 4.4** Transverse autocorrelation for process with $L_0$ = 10 m. Theory (solid curve) compared to ensemble average of 500 realizations (dots), using 1024 point realizations. Step size is equal to 100 m.

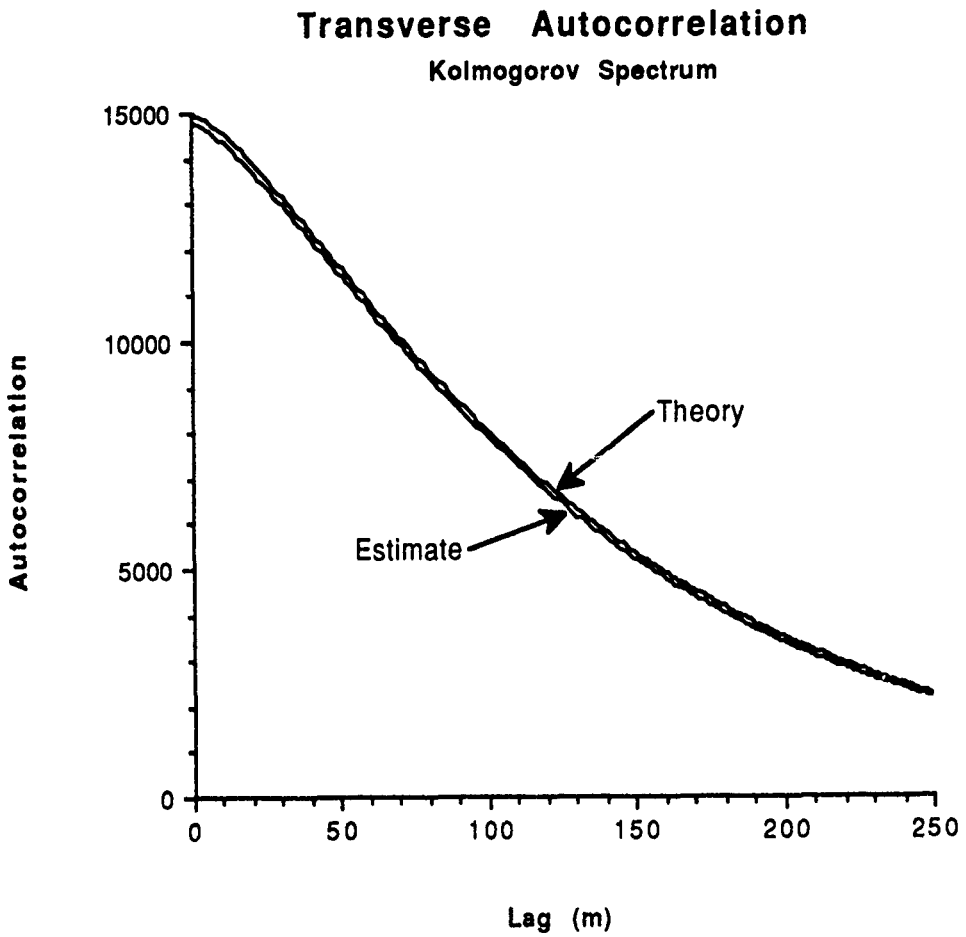


**Figure 4.5** Transverse autocorrelation for process with $L_0$ = 100 m. Theory compared to ensemble of 5000 realizations, using 1024 points. Step size is equal to 100 m.

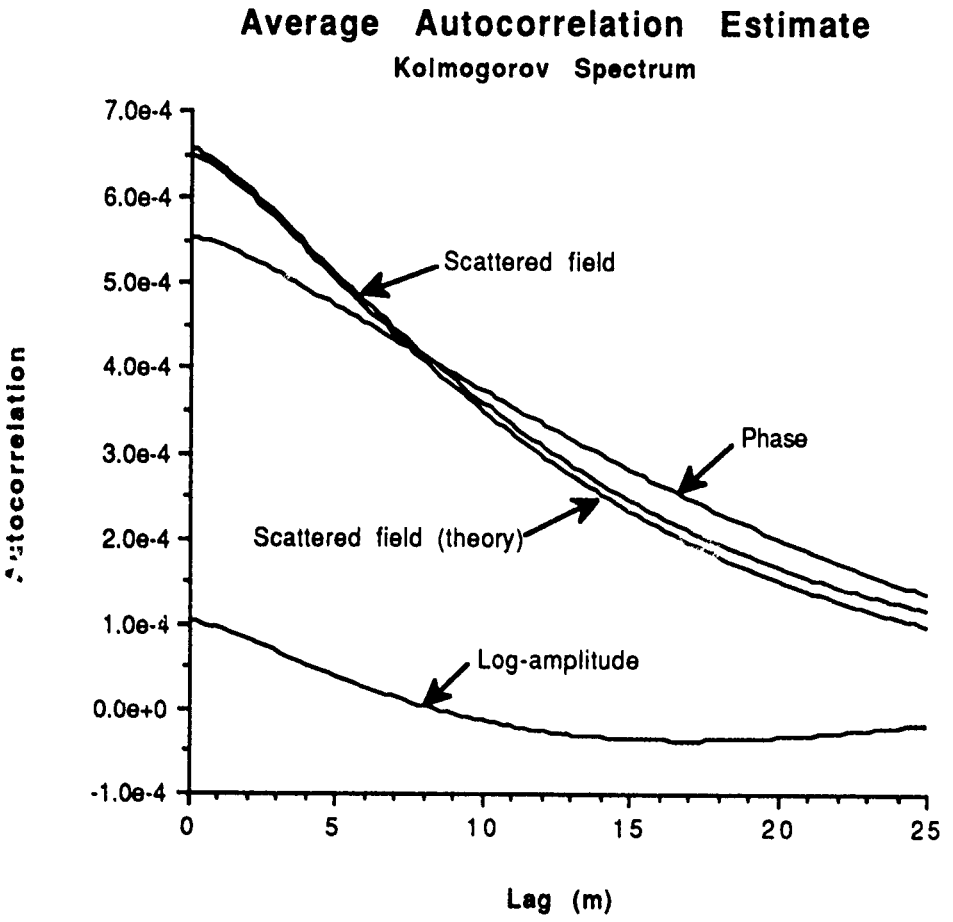


**Figure 4.6** Autocorrelations of field that has propagated through a medium with a Kolmogorov spectrum. Medium of variance $10^{-12}$ and outer scale 10 m are probed by 3.3-GHz plane wave. Theoretical scattered field autocorrelation is compared to numerical result. Phase and log-amplitude autocorrelations are also shown. Statistics are based on an ensemble average over 250 realizations. Each realization had forty-nine equally spaced phase screens of 1024 points and a vertical sampling interval of 0.2381 m. Read 7.0e–4 as $7 \times 10^{-4}$.

tion approach. Finally, the modified spectra are used to calculate the transverse spectra necessary for parabolic equation simulations.

### 4.4.1 Approach of Levy and Craig

The random index of refraction $n_f$ is inhomogeneous and possibly anisotropic in the atmospheric surface layer. Unfortunately, the spectral filtering method for generating realizations is limited to homogeneous processes and hence inapplicable. To circumvent these difficulties, Levy and Craig define an intermediate process $\xi = n_f / C_n$. They then make the simplifying assumption that $\xi$ is statistically homogeneous and isotropic and therefore can be simulated using spectral filtering. By assuming $\delta x \gg L_0$, they generate independent one-dimensional realizations of $\xi$ at uniform range steps. They use the one-dimensional form of the Kolmogorov spectrum $V_n$ that shows a $K^{-5/3}$ frequency dependence to design the spectral filter (Eq. 2.1) and then the produce realizations using the algorithm in Appendix A. The fluctuating index of refraction is recovered by $n_f = C_n \xi$. Numerical propagation studies are presented without comparison to theory.

The main error made by Levy and Craig is in selecting the wrong spectrum to generate realizations. The quantity of relevance to parabolic simulations is the integrated refractive index fluctuations (Eq. 3.4b); consequently, realizations should be generated using the transverse spectrum $S_t$ (Eq. 4.7). For turbulent fluctuations, $S_t$ exhibits a $K^{-8/3}$ frequency dependence in the inertial subrange rather than the $K^{-5/3}$ power law used by Levy and Craig. Selecting the wrong spectrum also introduces errors in scaling and dimensionality. (The one-dimensional spectrum $V_n$ has dimensions of meters, whereas $S_t$, like $S_n$, has dimensions of meters cubed.)

### 4.4.2 Modified Spectral Models for Surface Layer Turbulence

Levy and Craig define an (incorrect) intermediate process and then assume it is stationary. A more fundamental approach is to return to the three-dimensional spectral model for the turbulence and then determine what properties it must possess to force an appropriately defined intermediate process to be stationary. In this section, two possible models for boundary layer turbulence are considered that might be numerically tractable. Both models treat the spectral bandwidth as a height-independent constant. One approach considers the height-dependent structure constant to be a separable, deterministic function. The second model treats the turbulence as a quasi-nonogeneous process. In section 4.4.3, the transverse spectra for both models are discussed.

We begin with the standard one-dimensional spectrum for inhomogeneous, height-dependent, surface layer turbulence

$$V_n(K;z) = 0.124\, C_n^2(z)\, K^{-5/3}, \tag{4.18}$$

where the structure constant $C_n^2$ can be written in terms of the turbulent outer scale and the gradient of the mean profile (Eq. 2.9). For wave propagation studies, the

full three-dimensional spectrum is required. Assuming the medium is isotropic, the three-dimensional Kolmogorov spectrum follows from Equation 2.1:

$$S_n(K;z) = 0.033 C_n^2(z) K^{-11/3}. \tag{4.19}$$

Although it is not often mentioned in the atmospheric literature, spectral representations such as those given in Equation 4.19 are limited to frequencies in the inertial subrange. From section 2, the inertial subrange is defined by spatial frequencies within the band $2\pi / L_0 < K < 2\pi / \ell_0$. In the surface layer, however, the outer scale $L_0$ is itself a function of height through Equation 2.10. Hence we have the cumbersome situation where both the amplitude (through $C_n^2$) and the lower break frequency ($2\pi / L_0$) of the surface layer spectrum are dependent on height. For example, inferring an inhomogeneous von Karman spectrum directly from Equations 2.5 and 4.19 yields

$$S_n(K;z) = 0.033 C_n^2(z) \exp(-K^2 / K_m^2)\left[(K^2 + L_0^{-2}(z)\right]^{-11/6}. \tag{4.20}$$

Following the procedure of section 4.3, an inhomogeneous transverse spectrum can presumably be derived. But since the lower break frequency of the spectrum will depend on height, realizations of the transverse process cannot be generated using the filtered white noise approach detailed in Appendix A.

As a first approximation, we retain the height dependence through $C_n^2$ but replace the explicit $L_0(z)$ in Equation 4.20 with a height-independent constant $L_c$. This is probably reasonable, since we are primarily interested in the inertial subrange of turbulence and in this regime the only height dependence appears in $C_n^2$. In making this approximation, the spectral bandwidth of the inertial subrange is made height independent. To estimate an appropriate numerical value for $L_c$, one possible approach is to relate it to the variance of the index of refraction. This is detailed in Appendix B.

There is a second problem with the hypothesized spectrum in Equation 4.20. This inhomogeneous spectrum can presumably be related to a structure function or an autocorrelation by an appropriate transform pair. These are two-point statistical quantities, but Equation 4.20 depends on only a single height $z$. A more general model would show the explicit two-point dependence.

With these two conditions in mind, we hypothesize a modified three-dimensional spectral model for turbulence as

$$S_n(K;z_1,z_2) = \zeta(z_1,z_2)\Phi_n(K), \tag{4.21}$$

where

$$\Phi_n(K) = \exp(-K^2/K_m^2)(K^2 + L_c^{-2})^{-11/6}. \tag{4.22}$$

This model partitions the turbulence into a height-independent spectrum $\Phi_n$ and the quantity $\zeta(z_1,z_2)$, which in general depends on two heights. There is some latitude in defining $\zeta$, but it should be chosen to be consistent with existing meteorological expressions. We will consider two possible models. In the first, the structure constant is treated as a deterministic quantity. The ambiguous term $C_n^2(z)$ is separated to show explicit two-point dependence:

$$\zeta(z_1,z_2) = 0.033 C_n(z_1) C_n(z_2). \tag{4.23a}$$

Note that at $z_1 = z_2$, Equation 4.23a is consistent with the standard representations in Equations 4.18 and 4.19.

A second model treats the medium as being quasi-homogeneous. The two-point statistics of a quasi-homogeneous process can be written as the product of a term depending on the difference coordinate and a term depending on the average position. The spectrum $\Phi_n$ is the Fourier transform of the difference coordinate component, and hence $\zeta$ is written as

$$\zeta(z_1,z_2) = 0.033 C_n^2[(z_1+z_2)/2]. \tag{4.23b}$$

The component of a quasi-homogeneous process that depends on the average coordinate is generally a slowly varying function of its argument. Turbulent media are often modeled as quasi-homogeneous processes in theoretical wave propagation studies.[4,7,26]

For either model, it is useful to define the autocorrelation of the medium by an inverse transform,

$$\left\langle n_f(x_1,y_1,z_1) n_f(x_2,y_2,z_2) \right\rangle \equiv B_n(x_d,y_d,z_d;z_1,z_2)$$

$$= \zeta(z_1,z_2) \int_{-\infty}^{\infty} d\mathbf{K}\, \Phi(\mathbf{K}) \exp(i\mathbf{K}\cdot\mathbf{r}), \tag{4.24}$$

where $\mathbf{K} = (k_x, k_y, k_z)$ and $\mathbf{r} = (x_d, y_d, z_d)$. This formulation is useful for calculating the transverse spectrum for inhomogeneous media. The inverse transform is evaluated in Appendix B.

### 4.4.3 Transverse Spectrum

The pertinent statistical quantities for parabolic equation simulations are the autocorrelation of the integrated refractive index fluctuations $\phi_t$ and the associated transverse spectrum. Using Equations 4.4b and 4.24, and again assuming the step size is large compared to the correlation length, it follows that

$$\langle \phi_t(z_1)\phi_t(z_2)\rangle = \delta x \int_{-\infty}^{\infty} dx_d\, B_n(x_d, y_d = 0, z_d; z_1, z_2)$$

$$= \delta x \zeta(z_1, z_2) \int_{-\infty}^{\infty} dk_y \int_{-\infty}^{\infty} dk_z' \Phi(k_x = 0, k_y, k_z') \exp(ik_z' z_d)\,. \tag{4.25}$$

Equation 4.25 is valid for either form of $\zeta(z_1,z_2)$. We now consider the separable model of Equation 4.23a. It is useful to define the intermediate function,

$$\xi(z) = (0.033)^{-1/2} \phi_t(z) / C_n(z). \tag{4.26}$$

Since $\zeta$ is deterministic in this model, it can be brought inside the ensemble averaging brackets and

$$\langle \xi(z_1)\xi(z_2)\rangle = \delta x \int_{-\infty}^{\infty} dk_y \int_{-\infty}^{\infty} dk_z' \Phi(k_x = 0, k_y, k_z') \exp(+ik_z' z_d)$$

$$\equiv B_\xi(z_1 - z_2). \tag{4.27}$$

The autocorrelation of $\xi$ depends solely on the difference coordinate; hence the intermediate process is statistically homogeneous. Taking the Fourier transform gives the spectrum $S_\xi$:

$$S_\xi(k_z) \equiv \frac{(2\pi)^2}{(k_z^2 + L_0^{-2})^{4/3}} \delta x\, \pi^{1/2} \frac{\Gamma(4/3)}{\Gamma(11/6)}. \tag{4.28}$$

This spectrum can be used with the algorithm in Appendix A to generate realizations of $\xi$. Realizations of $\phi_t$ that are necessary for the parabolic equation simulations are recovered via Equation 4.26.

# 5. SUMMARY AND SUGGESTIONS FOR FURTHER WORK

Based on the analysis and numerical results of the preceding sections, we can conclude that the parabolic equation/split-step algorithm is a viable approach for modeling electromagnetic propagation through atmospheric turbulence. The propagation studies presented in this report were generated independently from TEMPER. It is a relatively simple task to design a subroutine that would also add "randomness" to the existing TEMPER code; all that is required is an appropriate spectral model, a random number generator, and access to a fast Fourier transform routine. The procedure should produce reliable results in an ensemble sense; the correct second-order statistics of the propagating field can be predicted by averaging across many realizations. As used in this report, spectral modeling assumes Gaussian statistics for the random medium. Consequently, the method is incapable of modeling low-probability events governed by non-Gaussian statistics.

The specific conclusions are summarized as follows:

1. Although the parabolic equation method has previously been used to study optical and acoustical propagation through random media, microwave propagation presents a unique set of problems. Since the perturbations to the field are relatively small, weak scattering theory can usually be used to estimate the propagating field. The inhomogeneous and possibly anisotropic nature of surface layer turbulence must be considered for low-altitude propagation.

2. Two-dimensional models like TEMPER are probably adequate for calculating the statistical moments of the propagating field. They may not, however, suffice for calculation of the log-amplitude fluctuations except in the very far field. The term "far field" itself has different interpretations in two and three dimensions.

3. Provided that the step size is large compared to the turbulent outer scale, the medium can be modeled by uncorrelated random phase screens. The relevant statistical quantity for generating the phase screens is the transverse spectrum. For homogeneous isotropic turbulence in the inertial subrange, the transverse spectrum shows a $K^{-8/3}$ frequency dependence. This is in contrast to the one-dimensional spectrum with a $K^{-5/3}$ power law used by Levy and Craig.

4. The transverse spectrum of homogeneous isotropic turbulence can be expressed in terms of a confluent hypergeometric function (Eq. 4.12). At microwave frequencies, a small argument approximation can be used to show the $K^{-8/3}$ behavior in the inertial subrange (Eq. 4.13). For a statistically homogeneous medium, the transverse autocorrelation can be evaluated and expressed using a modified Bessel function (Eq. 4.15).

5. Turbulence is inhomogeneous in the surface layer comprised of altitudes less than approximately 100 m. Both the structure constant and the outer scale depend on height. Since the outer scale determines the lower spatial frequency bound of the inertial subrange (Fig. 3.1), the implication is a spectrum where both the amplitude and the bandwidth depend on altitude. Such a spectrum is incompatible with the parabolic equation/split-step algorithm. As an approximation, the bandwidth was made constant and independent of height. Two plausible forms of the structure constant were considered. In one model, the structure constant was

treated as a separable, deterministic function. In the second model, the structure constant was treated as a quasi-homogeneous function.

The expressions derived for the transverse spectra and autocorrelations derived in section 4 are amenable to numerical implementation. A limited number of independent simulations were presented in this report. A possible program validating the proposed algorithm when coupled with TEMPER is outlined below:

1. Classical results for the canonical problems should be used as benchmarks in validating the computer routines. Analytical solutions are available for point source and plane wave propagation. Since these pristine solutions neglect interaction with deterministic refractive index profiles and rough surfaces, these features should be "turned off" when first testing randomness in TEMPER.

2. Initial numerical tests for both the plane wave and point source problems might best be done by assuming a Gaussian spectrum for the medium. Because a Gaussian spectrum is characterized by a single scale size, the resulting realizations do not exhibit the detailed fine structure of processes with power-law spectra (Fig. 4.3). Consequently, Monte Carlo simulations should converge relatively rapidly. Agreement with the simulations presented in section 4.2 should be expected.

3. The second set of tests for both the plane wave and the point source can be conducted for homogeneous isotropic turbulence. The effect of varying the numerical values of the various parameters (outer scale, "universal constants," etc.) can be studied. Required sampling rates can be defined, and the number of realizations necessary for convergence of the ensemble averages can be estimated. The numerical experiments presented in section 4.3 should be replicated.

4. Finally, the full features of TEMPER can again be "turned on." The structure constant for representative atmospheric profiles can be calculated. Realizations of inhomogeneous surface layer turbulence can be generated and included in TEMPER. The variance of the propagating field can be estimated. Numerical results should ultimately be compared to experimental observations.

Beyond the simple expedient of adding atmospheric randomness to TEMPER, this work has suggested directions for continued research:

1. Independent from TEMPER, additional simulations should be done for the point source problem. The analysis comparing the two- and three-dimensional problems should also be repeated for this configuration.

2. A good three-dimensional spectral model for boundary layer turbulence is needed. For a lack of quantitative data, the emphasis in this report is on isotropic models. Boundary layer turbulence is surely anisotropic, with relatively long correlation lengths in the horizontal. It would also be of interest to analyze the effect anisotropy would have on the various statistics of the field.

3. Numerical techniques could be developed for simulating quasi-homogeneous random media. It seems likely that an algorithm could be developed that would parallel that used for homogeneous media in Appendix A. Such an algorithm would also be of interest to researchers working in rough surface scattering.

4. Fractals appear to be a promising method for simulating turbulence; their most attractive feature is the ability to model intermittency. A good appreciation of atmospheric dynamics is needed to understand the role of intermittency and how it should be modeled with fractals. Further analytical work is necessary to predict the properties of a wave propagating through a fractal medium.

5. To validate an upgraded version of TEMPER containing turbulent fluctuations, the philosophy of this report has been to compare the numerical

results to established theoretical solutions. Only theoretical solutions to relatively simple problems have been considered, such as plane wave and point source propagation. Solutions to other problems are available in the literature; for example, Ishimaru[4] considers the propagation of a Gaussian beam. Path integral methods that reportedly combine large-scale deterministic features with randomness might be adapted to our purposes.[27,28] Modal techniques for propagation through deterministic profiles perhaps could be modified to include randomness.

6. At microwave frequencies, the turbulence possesses structure on the same scale as the wavelength. It is possible that this would induce polarization effects that are ignored in our scalar model. If possible, the magnitude of these effects should at least be estimated. It is unclear whether these features could be included in TEMPER.

## REFERENCES


[1]G. D. Dockery, *Description and Validation of the Electromagnetic Parabolic Equation Propagation Model (EMPE)*, JHU/APL FS-87-152, Applied Physics Laboratory, Laurel, Md. (1987).

[2]J. R. Kuttler and G. D. Dockery, "Theoretical Description of the Parabolic Approximation/Fourier Split-Step Method of Representing Electromagnetic Propagation in the Atmosphere," *Radio Sci.* **26**, 381-394 (1991).

[3]M. F. Levy and K. H. Craig, "Millimetre-Wave Propagation in the Evaporation Duct," in *Atmospheric Propagation in the UV, Visible, IR and MM-Wave Region and Related Systems Aspects*, AGARD Conf. Proc. 454, Neuilly-sur-Seine, France, pp. 26.1-26.10 (1989).

[4]A. Ishimaru, *Wave Propagation and Scattering in Random Media*, Academic Press, New York (1978).

[5]A. J. Devaney, "The Inverse Problem for Random Sources," *J. Math. Phys.* **20**, 1687-1691 (1979).

[6]B. J. Uscinski, *The Elements of Wave Propagation in Random Media*, McGraw-Hill, New York (1978).

[7]V. I. Tatarskii, *The Effects of the Turbulent Atmosphere on Wave Propagation*, Keter Press, Jerusalem (1971).

[8]H. A. Panofsky and J. A. Dutton, *Atmospheric Turbulence. Models and Methods for Engineering Applications*, John Wiley and Sons, New York (1984).

[9]Z. Sorbjan, *Structure of the Atmospheric Boundary Layer*, Prentice Hall, Englewood Cliffs, N. J. (1989).

[10]D. E. Kerr (ed.), *Propagation of Short Radio Waves*, Dover, New York (1951).

[11]E. E. Gossard, "Clear Weather Meteorological Effects on Propagation at Frequencies above 1 GHz," *Radio Sci.* **16**, 589-608 (1981).

[12]E. E. Gossard, "Refractive Index Variation and Its Height Distribution in Different Air Masses," *Radio Sci.* **12**, 89-105 (1977).

[13]S. D. Burk, "Temperature and Humidity Effects on Refractive Index Fluctuations in Upper Regions of the Convective Boundary Layer," *J. Appl. Meteorol.* **20**, 717-721 (1981).

[14]E. L. Andreas, "Estimating $C_n^2$ Over Snow and Sea Ice from Meteorological Data," *J. Opt. Soc. Am. A: Opt. Image Sci.* **5**, 481-495 (1988).

[15]A. S. Monin and A. M. Yaglom, *Statistical Fluid Mechanics*, MIT Press, Cambridge, Mass. (1971).

[16]E. E. Gossard, "The Height Distribution of Refractive Index Structure Parameter in an Atmosphere Being Modified by Spatial Transition at Its Lower Boundary," *Radio Sci.* **13**, 489-500 (1978).

[17]T. E. Van Zandt, J. L. Green, K. S. Gage, and W. L. Clark, "Vertical Profiles of Refractivity Turbulence Structure Constant: Comparison of Observations by the Sunset Radar with a New Theoretical Model," *Radio Sci.* **13**, 819-829 (1978).

[18]M. R. Battaglia, *Modelling the Radar Evaporative Duct*, Department of Defence, Defence Science and Technology, RAN Research Laboratory, Australia (1985).

[19]C. Macaskill and T. E. Ewart, "Computer Simulation of Two-Dimensional Random Wave Propagation," *IMA J. Appl. Math.* **33**, 1-15 (1984).

[20]A. Papoulis, *Probability, Random Variables, and Stochastic Processes*, McGraw-Hill, New York (1984).

[21]D. Rouseff, K. B. Winters, and T. E. Ewart, "Reconstruction of Oceanic Microstructure by Tomography," *J Geophys. Res* **96**, 8823-8834 (1991).

[22]T. E. Ewart, "A Model of the Intensity Probability Distribution for Wave Propagation in Random Media," *J. Acoust Soc Am* **86**, 1490-1498 (1989).

[23]E. Jakeman, "Scattering by Gamma-Distributed Phase Screens," *Waves in Random Media* **2**, 153-167 (1991).

[24]Y. Kim and D. L. Jaggard, "Band-Limited Fractal Model of Atmospheric Refractivity Fluctuation," *J. Opt Soc Am A Opt Image Sci.* 5, 475-481 (1988)

[25]D. L. Jaggard, "On Fractal Electrodynamics," in *Recent Advances in Electromagnetic Theory*, H. N. Kritikos and D. L. Jaggard (ed.), Springer-Verlag, New York (1991).

[26]S. M. Rytov, Y. A. Kravtsov, and V. I. Tatarskii, *Principles of Statistical Radiophysics*, Vol. 4, Springer-Verlag, New York (1989).

[27]S. M. Flatté, R. Dashen, W. H. Munk, K. M. Watson, and F. Zachariasen, *Sound Transmission Through a Fluctuating Ocean*, Cambridge University Press, New York (1979).

[28]S. M. Flatté, "Wave Propagation through Random Media: Contributions from Ocean Acoustics," *Proc. IEEE* **71**, 1267-1294 (1983).

[29]I. S. Gradshteyn and I. M. Ryzhick, *Tables of Integrals, Series and Products*, Academic Press, Orlando, Fla., p. 490 (1980).

[30]H. W. Ko, J. W. Sari, and J. P. Skura, "Anomalous Microwave Propagation through Atmospheric Ducts," *Johns Hopkins APL Tech. Dig.* **4**, 12-26 (1983).

[31]M. Spivack, "Accuracy of the Moments from Simulation of Waves in Random Media," *J. Opt. Soc. Am. A* **7**, 790-793 (1990).

[32]D. Rouseff and R. P. Porter, "Diffraction Tomography and the Stochastic Inverse Scattering Problem," *J. Acoust. Soc. Am.* **89**, 1599-1605 (1991).

[33]J. M. Martin and S. M. Flatté, "Intensity Images and Statistics from Numerical Simulation of Wave Propagation in 3-D Random Media," *Appl. Opt.* **27**, 2111-2127 (1988).

[34]W. H. Press, B. P. Flannery, S. A. Teukolsky, and W. T. Vetterling, *Numerical Recipes*, Cambridge University Press, Cambridge, England (1986).

[35]A. V. Oppenheim and R. V. Schafer, *Digital Signal Processing*, Prentice-Hall, Englewood Cliffs, N. J. (1975).

[36]T. E. Ewart and S. A. Reynolds, "Experimental Ocean Acoustic Field Moments versus Predictions," in *Ocean Variability and Acoustic Propagation*, J. Potter and A. Warn-Varnas (ed.), Kluwer Academic Publishers, Boston, Mass., pp. 23-40 (1991).

[37]M. Abramowitz and I. M. Stegun, *Handbook of Mathematical Functions*, National Bureau of Standards, Washington, D. C. (1965).

[38]K. H. Craig and M. F. Levy, "Parabolic Equation Modelling of the Effects of Multipath and Ducting on Radar Systems," *IEE Proc. F* **138**, 153-162 (1991).

# APPENDIX A.

## GENERATING RANDOM REALIZATIONS

Realizations of atmospheric turbulence can be simulated in various ways. The most complete method is to solve the governing Navier-Stokes equations describing the fluid motion numerically. Unfortunately, this procedure is not feasible at the large scales necessary for wave propagation studies. As an alternative, we are left with numerical techniques that produce realizations consistent with some order (usually second) of the statistics describing the medium. While these methods yield realizations exhibiting the correct statistics, the individual realizations may or may not actually "look" like the true process. As a result, these methods are best used as part of an algorithm where the entire procedure (in this case, wave propagation through a random medium) is simulated many times and then the statistics are inferred by averaging across an ensemble of realizations. These procedures fall under the general heading of Monte Carlo techniques.

One of the first studies of wave propagation through random media using the parabolic equation was conducted by Macaskill and Ewart.[A1] Following their example, most subsequent studies have simulated realizations of the random medium using spectral filtering. In this approach, realizations of Gaussian white noise are first generated using a random number generator and then filtered. To obtain the desired output process, the filter is designed based on the square root of the desired spectrum.[A2] An efficient algorithm based on the fast Fourier transform (FFT) is now presented. This approach is particularly attractive in the present context, since the FFT is already used in the parabolic equation/split-step algorithm.

Consider an $N$ point process $\phi_t[\ell]$ defined by

$$\phi_t[\ell] \equiv \phi_t(\ell\,\delta z), \qquad \ell = 0,1,\ldots N-1, \tag{A1}$$

where the square brackets indicate a sampled version of the continuous process and the sampling interval is $\delta z$. The discrete spectrum is a sampled version of the continuous spectrum

$$\begin{aligned} S_t[j] &= (\delta z)^{-1} S_t\big(j/(N\delta z)\big), && j = 0,1,\ldots N/2 \\ S_t[j] &= (\delta z)^{-1} S_t\big((N-j)/(N\delta z)\big), && j = N/2,\ldots (N-1). \end{aligned} \tag{A2}$$

The discrete realization is recovered via an inverse discrete transform,

$$\phi_t[\ell] = N^{-1} \sum_{j=0}^{N-1} \tilde{\phi}_t[j] \exp\left[-i2\pi j\ell/N\right], \tag{A3}$$

where the spectral components are generated according to the rule

$$\begin{aligned} \tilde{\phi}_t[j] &= \left[-S_t[j]N \ln(q_j)\right]^{1/2} \exp(i2\pi r_j) && \text{for } j \neq 0,\ j \neq N/2 \\ \tilde{\phi}_t[j] &= \left[-S_t[j]2N \ln(q_j)\right]^{1/2} \cos(2\pi r_j) && \text{for } j = 0 \text{ or } j = N/2. \end{aligned} \tag{A4}$$

---

[A1] C Macaskill and T E Ewart, "Computer Simulation of Two Dimensional Random Wave Propagation," *IMA J Appl Math* 33, 1-15 (1984)

[A2] A Papoulis, *Probability, Random Variables, and Stochastic Processes*, McGraw-Hill, New York (1984)

In Equation A4, $q_j$ and $r_j$ are random numbers uniformly distributed between zero and 1. Note that both the zero frequency and the Nyquist component are purely real. To make the realization purely real, there is the additional symmetry constraint that

$$\begin{aligned} q_j &= q_{N-j}, \qquad j = 1,2,\ldots N/2 \\ r_j &= r_{N-j}, \qquad j = 1,2,\ldots N/2. \end{aligned} \tag{A5}$$

The inverse transform in Equation A3 is efficiently evaluated using an FFT. The resulting realization of the process is purely real. A marginal increase in efficiency can be gained by relaxing the symmetry constraint, generating a complex $\phi_l$, and then treating the real and imaginary parts as independent realizations.[A3] Explicit evaluation of the probability integrals shows that this algorithm produces realizations with the desired spectrum.

[A3] J. M. Martin and S. M. Flatté, "Intensity Images and Statistics from Numerical Simulation of Wave Propagation in 3-D Random Media," *Appl. Opt.* 27, 2111-2127 (1988)

## REFERENCES


[A1]C. Macaskill and T. E. Ewart, "Computer Simulation of Two-Dimensional Random Wave Propagation," *IMA J. Appl. Math.* **33**, 1-15 (1984).

[A2]A. Papoulis, *Probability, Random Variables, and Stochastic Processes*, McGraw-Hill, New York (1984).

[A3]J. M. Martin and S. M. Flatté, "Intensity Images and Statistics from Numerical Simulation of Wave Propagation in 3-D Random Media," *Appl. Opt.* **27**, 2111-2127 (1988).

# APPENDIX B.

## VARIANCE OF REFRACTIVE INDEX IN THE SURFACE LAYER

As discussed in section 2., atmospheric turbulence is typically modeled as a locally homogeneous random process; as such, it must be characterized by a structure function rather than an autocorrelation. In the frequency domain, the locally homogeneous character is reflected in the spectrum being undefined for the low spatial frequencies in the energy input regime. For mathematical convenience, however, a spectral shape is often assigned, making an inverse transform possible, and hence a function that can be interpreted as an autocorrelation.

In section 4.4.3, a model for surface layer turbulence was developed. A parameter $L_c$ was defined with units of meters, where the upper bound of the energy input regime was defined by $2\pi/L_c$. One method for assigning a numerical value to $L_c$ is to examine its relationship to the variance of the medium. To calculate the variance, we must first calculate the autocorrelation.

The autocorrelation was related to the spectrum in Equation 4.24. If the spectrum is isotropic, the three-dimensional integral can be converted to a single integral,[B1] and

$$B_n(r_d;z_1,z_2)=\zeta(z_1,z_2)4\pi r_d^{-1}\int_0^\infty \Phi(K)K\sin(Kr_d)dK. \qquad \text{(B1)}$$

Let $z \equiv z_1 = z_2$. Substituting the spectrum into (B1), neglecting the exponential term, and evaluating the resulting integral yields[B2]

$$B_n(r_d;z)=0.391C_n^2(z)L_c^{2/3}(r_dL_c^{-1}/2)^{1/3}K_{1/3}(r_dL_c^{-1}). \qquad \text{(B2)}$$

The variance is derived by evaluating Equation B3 at $r_d = 0$:

$$\sigma_n^2 \equiv B_n(r_d=0)=0.523C_n^2(z)L_c^{2/3}. \qquad \text{(B3)}$$

Hence the variance of the medium is proportional to $L_c^{2/3}$. The structure constant $C_n^2(z)$ is given by Equation 2.9.

---

[B1] A Ishimaru, *Wave Propagation and Scattering in Random Media*, Academic Press, New York, p 517 (1978)

[B2] I S Gradshteyn and I M Ryzhick, *Tables of Integrals, Series and Products*, Academic Press, Orlando, Fla (1980)

## REFERENCES

[B1] A. Ishimaru, *Wave Propagation and Scattering in Random Media*, Academic Press, New York, p. 517 (1978).

[B2] I. S. Gradshteyn and I. M. Ryzhick, *Tables of Integrals, Series and Products*, Academic Press, Orlando, Fla. (1980).

# INITIAL DISTRIBUTION EXTERNAL TO THE APPLIED PHYSICS LABORATORY*

The work reported in TG 1381 was done under Navy Contract N00039-89-C-5301 and is related to Task BKAW9BXX, supported by NAVSEA.

| ORGANIZATION | LOCATION | ATTENTION | No. of Copies |
|---|---|---|---|
| DEPARTMENT OF DEFENSE | | | |
| Office of the Under Secretary of Defense, Research and Engineering | Washington, DC 20301 | Accessions | 1 |
| Defense Technical Information Center | Alexandria, VA 23314 | Accessions | 12 |
| Defense Advanced Research Projects Agency | Arlington, VA 20331 | Accessions | 1 |
| DEPARTMENT OF THE NAVY | | | |
| Chief of Naval Operations | Washington, DC 20350 | Accessions | 2 |
| COMOPTEVFOR | Norfolk, VA 23511-6388 | Library | 1 |
| Naval Air Development Center | Warminster, PA 18974-5000 | Library | 1 |
| FCDSSA, Dam Neck | Virginia Beach, VA 23461-5300 | Library | 1 |
| Office of the Assistant Secretary of the Navy | Washington, DC 20350 | Accessions | 2 |
| Office of Naval Research | Arlington, VA 22217 | Library | 2 |
| Office of Naval Technology | Arlington, VA 22209 | Library | 2 |
| Naval Air Systems Command | Washington, DC 22202 | Library, Air 7226 | 2 |
| Naval Electronic Systems Command | Arlington, VA 20360 | Library | 2 |
| Naval Postgraduate School | Monterey, CA 92940 | Library | 2 |
| Naval Research Laboratory | Washington, DC 20375 | Library | 2 |
| Space & Naval Warfare Systems Command | Washington, DC 20360 | Library | 1 |
| Naval Sea Systems Command | Washington, DC 22202 | Library, Sea 9961 | 2 |
| Naval Ship Weapon Systems Engineering Station | Fort Hueneme, CA 93043-5007 | Library | 2 |
| Naval Avionics Center | Indianapolis, IN 46219-2189 | Library | 2 |
| Naval Surface Weapons Center | Dahlgren, VA 22448 | Library | 2 |
| Naval Weapons Center | China Lake, CA 93555 | Library | 2 |
| Naval Surface Warfare Center | White Oak, MD 20903 | Library | 2 |
| Pacific Missile Test Center | Pt. Mugu, CA 93042 | Director of Research | 2 |
| U.S. Naval Academy | Annapolis, MD 21402 | Library | 2 |
| NAVTECH REP | Laurel, MD 20723-6099 | | 2 |
| SPAWAR | Arlington, VA 20363-5100 | Library | 2 |
| Naval Weapon Support Center | Crane, IN 47522 | Library | 2 |
| Naval Ocean Systems Center | San Diego, CA 92152 | Library | 1 |
| DEPARTMENT OF THE ARMY | | | |
| Ballistic Missile Defense Advanced Technology Center | Huntsville, AL 35807 | Library | 1 |
| Missile Command | Huntsville, AL 35898 | Library | 1 |
| Commander, Chemical Research, Development and Engineering | Aberdeen Proving Ground, MD 21010-5423 | B. E. Stuebing | 1 |
| DEPARTMENT OF THE AIR FORCE | | | |
| Air Force Avionics Laboratory Aeronautical Systems Division | Wright-Patterson AFB, OH 45433-6503 | Library | 2 |
| OTHERS | | | |
| Applied Physics Laboratory University of Washington | Seattle, WA 98105-6698 | P. Kaczkowski | 1 |
| | Ocala, FL 32674 | R W. Hart | 1 |

Requests for copies of this report from DoD activities and contractors should be directed to DTIC, Cameron Station, Alexandria Virginia 22314, using DTIC Form 1 and, if necessary DTIC Form 55

*Initial distribution of this document within the Applied Physics Laboratory has been made in accordance with a list on file in the APL Technical Publications Group